Thesis/
Reports
Radke,
L. F.

AIRBORNE STUDIES OF THE SMOKES FROM A BOREAL BIOMASS FIRE IN ALASKA, 1990

AIRBORNE STUDIES..

WARD

Coop Agreement
University
of
Washington

CLOUD AND AEROSOL RESEARCH GROUP

AIRBORNE STUDIES OF THE SMOKES FROM
A BOREAL BIOMASS FIRE IN ALASKA, 1990

by

Lawrence F. Radke, Peter V. Hobbs, J. David Nance,
Krista K. Laursen, Ronald J. Ferek and Dean A. Hegg
Department of Atmospheric Sciences,
University of Washington,
Seattle, WA 98195

and

R. E. Weiss
Radiance Research, Seattle WA 98177

UNIVERSITY OF WASHINGTON
DEPARTMENT OF ATMOSPHERIC SCIENCES
SEATTLE, WASHINGTON
98195

AIRBORNE STUDIES OF THE SMOKES FROM A BOREAL BIOMASS FIRE IN ALASKA, 1990

by

Lawrence F. Radke, Peter V. Hobbs, J. David Nance,
Krista K. Laursen, Ronald J. Ferek and Dean A. Hegg
Department of Atmospheric Sciences,
University of Washington,
Seattle, WA 98195

and

R. E. Weiss
Radiance Research, Seattle WA 98177

Final Report to Intermountain Research Station,
Forest Service, U.S. Department of Agriculture, for #INT-89426-RJVA
July 1, 1990, through November 30, 1990

This research was supported in part by funds provided by the Defense Nuclear Agency,
under Project IACRO 89-903, Task RA, Work Unit 00024,
and the Intermountain Research Station, Forest Service,
U.S. Department of Agriculture

APRIL 1991

AIRBORNE STUDIES OF THE SMOKES FROM A BOREAL BIOMASS FIRE IN ALASKA, 1990

by

Lawrence F. Radke, Peter V. Hobbs, J. David Nance,
Krista K. Laursen, Ronald J. Ferek and Dean A. Hegg
Department of Atmospheric Sciences,
University of Washington,
Seattle, WA 98195

and

R. E. Weiss
Radiance Research, Seattle WA 98177

Final Report to Intermountain Research Station,
Forest Service, U.S. Department of Agriculture, for #INT-89426-RJVA
July 1, 1990, through November 30, 1990

This research was supported in part by funds provided by the Defense Nuclear Agency,
under Project IACRO 89-903, Task RA, Work Unit 00024,
and the Intermountain Research Station, Forest Service,
U.S. Department of Agriculture

TABLE OF CONTENTS

	Page
1. INTRODUCTION	1
2. DATA COLLECTION PROCEDURES AND ANALYTICAL METHODS	4
3. EMISSION FACTORS FOR SOME TRACE GASES AND PARTICULATE CHEMICAL SPECIES	10
4. PARTICLE SIZES AND TOTAL PARTICULATE EMISSIONS FACTORS	17
5. OPTICAL PROPERTIES OF THE SMOKE	21
6. SHAPES OF THE SMOKE PARTICLES	23
7. SCAVENGING OF THE SMOKE BY CLOUDS	25
8. SUMMARY	25
9. REFERENCES	27
10. ACKNOWLEDGEMENTS	30
APPENDIX: THE UNIVERSITY OF WASHINGTON'S CONVAIR C-131A RESEARCH AIRCRAFT AND THE INSTRUMENTS USED IN THIS STUDY	

AIRBORNE STUDIES OF THE SMOKES FROM A BOREAL BIOMASS FIRE IN ALASKA, 1990

1. INTRODUCTION

Background

It is becoming increasingly evident that the concentrations of various gases and particles in the atmosphere are being modified on a global scale by anthropogenic activities. Biomass burning plays an important role in this respect, although quantitative data, especially in a form relevant to global change issues, are scant. These uncertainties were highlighted in the Report of the Study of Man's Impact on Climate (SMIC, 1971), and a decade and a half later there are still "...no satisfactory published estimates of the amounts of biomass converted to gaseous and particulate matter" (National Academy of Sciences, 1986).

The Cloud and Aerosol Research (CAR) Group at the University of Washington (UW) has been studying the emissions from biomass burning since the 1960s. This work has led to new knowledge concerning the uncertainties in the quantity and characteristics of the emissions produced from fires in biomass fuels. In our earliest work we observed that forest fires were prolific sources of cloud condensation nuclei (CCN) (Hobbs and Radke, 1969). Since CCN concentrations modulate cloud droplet concentrations, cloud albedo and precipitation probability, their importance is clear, yet they are surprisingly poorly defined (e.g., Twomey, 1977; Radke 1989; Radke et al., 1990).

Much of our work during the 1970s and mid 1980s focused on smoke emissions from biomass fires in the Pacific Northwest (Eagan et al., 1974; Radke et al., 1978; Stith et al., 1981). The scope of our research broadened, both scientifically and geographically, in 1986 as we began to assist land management agencies in the development of new emissions data for smoke management purposes and the Department of Defense in the quantification of variables that are important to the "nuclear winter" hypothesis (Crutzen and Birks, 1982; Turco et al., 1983). This lead to our participation in several studies of biomass fires in

southern California and Ontario where we found that emissions can vary substantially from fire to fire or from location to location. For example, our studies of biomass fires that burned downwind of large urban areas in southern California have shown that some of the trace materials found in biomass smokes occur due to the resuspension of anthropogenically-produced materials that were previously deposited in the fuel bed (Hegg et al., 1987, 1990).

Other factors that may cause emissions to vary from one fire to another include the composition, moisture content, and spatial distribution of the fuel, and the supply of oxygen to the combustion zone. Hegg et al. (1988) found a striking difference in the quantities of ammonia emitted from two fires of essentially identical fuels differentiated only by the time of year (summer versus winter) during which they burned and the amount of rainfall received in the week preceding. Hegg et al. (1990) found clear relationships between emissions of smoke particles and methane and ratios of CO to CO_2 emissions. The CO to CO_2 ratio was found to vary according to concentrations of O_2 in the combustion zone.

Atmospheric conditions can play an important role in the atmospheric lifetime of smoke particles and certain water-soluble trace gases (e.g. ammonia) once they are emitted. In Ontario, we gained insights into the smoke particle scavenging efficiency of plume-capping cumulus clouds (Radke et al., 1991b).

Most of our previous studies have been of prescribed burns of forest slash. Because they have finite supplies of fuel, prescribed fires tend to burn through life cycles that consist of an initial flaming phase followed by a smoldering phase. Since each of these phases has distinctive characteristics (see, for example, Patterson and McMahon, 1984), key trace gas and particulate emissions can vary over wide ranges during the course of a prescribed fire. Thus, the extrapolation of emissions data from prescribed fires to describe the emissions from wildfires that burn uncontrolled under conditions that promote rapid fire spread may not be justified. Therefore, in an effort to increase the quantity of collected data

that describe wildfire emissions, and to achieve a greater level of geographical diversity in our measurements, we seized the opportunity to obtain our first measurements in the smoke plume of a boreal forest wildfire (Fire A121) in Alaska.

Site Description

Wildland fires in the State of Alaska, Yukon and Northwest Territories of Canada, and Siberia in the USSR contribute substantial quantities of trace gases (greenhouse gases) and particulate matter to the atmosphere each year. This fire phenomenon occurs seasonally and is often a major feature of the arctic region during the summer months. Remote villages are often threatened by high-intensity, fast moving wildfires that are virtually uncontrollable. Most fires in this region burn out naturally. The consequence in Alaska is the occurrence of wildland fires on nearly 1 million ha each year. From mid-June to mid-August of 1990, over 0.8 million ha either received modified suppression with no firefighters committed or was under limited suppression. The large area of fire created severe smoke problems affecting the general air quality of Alaska with concurrent related visibility and health problems. A paucity of smoke characteristics data makes it impossible to evaluate air quality and fire management alternatives that are driven by smoke management consideration in Alaska. For example, it is hypothesized that a gigantic smoke pall such as existed in the interior of Alaska can prolong drought conditions. This study initiated work to resolve some of the critical issues associated with smoke production from wildland fires in the interior of Alaska.

As part of a larger study being conducted by the Intermountain Research Station of the US Forest Service and the Defense Nuclear Agency , three airborne flights were initiated from Fairbanks to the Yukon Flats area (location coordinates 66° 37' N latitude and 147° 50' W longitude) for the purpose of characterizing the smoke emissions from Fire A121. The flights were coordinated by the Alaska Fire Service (Bureau of Land Management, National Park Service, Fish and Wildlife Service, Alaska Forest Service, and

other agencies). The experiment was initiated at the beginning of the severe Alaska fire episode on June 27–28, 1990 that extended for 8 weeks ending in late August.

Fire A121 was ignited on June 26 following a period of dry lightning in the Yukon River area approximately 160 km due north of Fairbanks, AK. A smoke jumper crew parachuted to the fire during the morning of June 27 and constructed a fireline along the southerly flank of the fire. The first emissions sampling flight (UW flight #1458) was flown on 27 June between 1700 and 2000 PDT. A121 was approximately 200 ha in size. During this flight, the smoke jumper crew reported that they had lost the fireline already constructed. A float plane arrived and ferried the smoke jumper crew out of the area. From this time forward, A121 was a free-burning fire only limited by prevailing weather and fuel conditions. The fire was burning in a decadent black spruce forest on reasonably level terrain along the alluvial plane region approximately 20 km north of the Yukon River. During flight #1458, single trees were torching with the fire spreading through ground litter fuels. Between 2000 and 2200 hours, immediately following the departure of the UW aircraft from the vicinity of A121, the fire jumped the partially completed control line and spread toward the southeast growing in size from 200 ha to over 2000 ha.

On the 28th of June 1990, two flights were made with the first from 1400 to 1730 PDT and the second from 1915 to 2300 PDT. A121 burned toward the northeast during the morning and afternoon of 28 June. A121 doubled in size on June 28, but at no time sustained a crown fire. The primary fire activity was a low-intensity ground fire burning in surface needle fuels with an occasional torching of crowns. The underlying litter and duff fuels were not dry enough to sustain combustion, resulting in a minor smoldering component to the emissions released.

2. DATA COLLECTION PROCEDURES AND ANALYTICAL METHODS

The measurements were made aboard the University of Washington's C-131 research aircraft. A wide range of instruments and a combination of continuous and "grab"

sampling techniques enabled us to measure several different trace gases and particulate species. Trace gas and particle mass concentrations were determined by collecting samples of air from the smoke plume in a 1.5 m^3 polyethylene bag aboard the aircraft. Portions of selected samples were drawn through each of a pair of 37 mm Teflon filters for purposes of measuring particle mass concentrations. The air passing through one of the filters in each pair was initially passed through a centrifuge to remove particles with aerodynamic diameters > 3.5 μm. The air passing through the other filter was unmodified. Thus, by measuring the flow of air through each filter, mass concentrations could be computed for fine particles (those with aerodynamic diameters < 3.5 μm) and for all particles after determining the difference in weight of each filter before and after its exposure to polluted air. (Many of the largest particles in the smoke plume were nevertheless removed in the bend of the sampling port and by settling within the polyethylene bag during the several minutes that were necessary to complete the measurements. The combination of these effects, in practice, place an upper size limit of approximately 50 μm on the particles that were collected on filters exposed to unmodified air.) Typically, fine particle mass concentrations measured from the filters that were exposed to pre-centrifuged air were about 90% of the "total" mass concentrations measured from filters exposed to unmodified air. Measured ratios of fine particle to total mass concentrations ranged from 0.83 to 1.03 for a total of 13 filter pairs.

A different set of (47 mm) Teflon filters were also exposed to the smoke samples collected in the 1.5 m^3 bag and used to measure concentrations of gaseous NH_3 and particulate NH_4^+, NO_3^- and $SO_4^=$ with a variety of techniques (see Appendix).

Separate portions of selected 1.5 m^3 bag samples were collected in previously evacuated stainless steel canisters for subsequent chemical analysis. The contents were analyzed for several trace constituents, including those carbonaceous gases necessary for the computation of emission factors. With the exception of CO_2, NO_x, O_3 and NH_3, all trace gases discussed in this report were measured from the samples contained in these

canisters. A total of ten canisters were analyzed for the Alaskan fire, however, only eight of these corresponded to air samples for which simultaneous particle mass concentrations were measured. The other two canisters contained samples of ambient air collected outside of the smoke plume. Analysis of the gases in the cans was performed by Dr. R. A. Rasmussen of the Oregon Graduate Institute of Science and Technology in Beaverton, Oregon. Among the techniques used by Dr. Rasmussen to analyze the can samples are gas chromatography, mass spectroscopy, and electron capture [see Rasmussen et al. (1974) and Rasmussen and Khalil (1980, 1981) for descriptions of these techniques].

CO_2 and NO_x were measured continuously on board the aircraft except on those occasions when the 1.5 m^3 bag was filled. During these times, CO_2 and NO_x were measured from the samples contained within the bag. The CO_2 instrument, a customized Teco Model 41H, was zeroed (using pure N_2) and spanned (using a gas of known CO_2 concentration) at least once during the course of each flight. The NO_x instrument, a modified Monitor Labs Model 8840, unfortunately, was not properly zeroed during any of the three flights in Alaska. We, therefore, chose the zero reading level as the minimum value of the returned signal after filtering out the noise. This resulted in background concentrations of NO_x of ~1 ppb. Background concentrations of NO_x reported by Logan (1983) for various sites and altitudes are in the sub-parts-per-billion range. Therefore, with plume concentrations of NO_x on the order of 30 ppb, the deviation of the true background concentration of NO_x from 1 ppb is unlikely to be significant. The NO_x instrument was calibrated in the laboratory against a permeation tube and span gas dilution system.

O_3 concentrations in the environment surrounding the aircraft were monitored continuously throughout the three flights. At no time did the O_3 instrument, a Monitor Labs Model 8410 A, sample off of the 1.5 m^3 bag. The O_3 instrument was also calibrated in the laboratory against an Environics 300 Series O_3 source (UV radiation).

We continuously monitored the optical coefficients for total light extinction (σ_e) and light extinction due to scattering (σ_s) by particles at visible wavelengths (540 nm) during

each of our passes through the plume from the Alaskan fire. For this purpose, we used an optical extinction cell (for measuring σ_e) operating in parallel with an integrating nephelometer (for measuring σ_s). From the measured values of these two quantities, we were able to compute the optical coefficient for extinction due to absorption by the smoke ($\sigma_a = \sigma_e - \sigma_s$) and the single scattering albedo ($\tilde{\omega} = \sigma_s/\sigma_e$) of the smoke. This system permitted real-time measurements with a time resolution of ~1 second (or about 80 meters of flight path). The integrating nephelometer was calibrated by comparing the instrument output when viewing clean (particle-free) air and Freon 12 with the expected σ_s values for these substances. Pre-flight calibration of the OEC/nephelometer system was accomplished by ensuring that $\tilde{\omega}$ did not deviate from unity for laboratory-generated non-absorbing particles (such as polyethylene glycol, NaCl, or $(NH_4)_2SO_4$) with an appropriate and known size distribution. This system has been used by us in numerous biomass fire studies since December of 1986.

The size spectra of smoke particles from 0.01–45 μm in diameter were measured with an array of five instruments all of which were fed from a common 90 liter batch sample of air (see Appendix). Several such samples were collected, many of which were concurrent with the 1.5 m^3 bag samples. At the core of this system is the PMS Model ASASP-X which measures the size distribution of particles in the accumulation mode (particles with diameters between 0.1 and 2.0 μm) where the vast majority of smoke particle mass resides. This instrument measures the amount of light scattered from a focused stream of particles as they pass through a laser beam and interprets the received signal in terms of its correspondence with that produced by the calibration source (latex spheres). On occasion, the laser in this instrument has been jolted out of proper alignment. When this occurs, the instrument is sent back to PMS for re-tuning and calibration. Subsequent periodic checking of the instrument's response to laboratory-generated, spherical particles of known size ensures that it is functioning properly. This instrument

was last tuned and calibrated by PMS on 30 March, 1990, just 3 months before this study was undertaken, and it appears to have performed quite well.

Emission factors (i.e. mass of species emitted into the atmosphere per unit mass of biomass burnt) were computed using the carbon-balance method (Ward et al., 1982; Radke et al., 1988). This method requires in-plume measurements of all major carbon-containing combustion products. These include CO_2 and CO, which are of primary importance, a less important subset of hydrocarbons (CH_4, C_2H_2, C_2H_6, C_3H_6, C_3H_8, and C_4 isomers), and the smoke particles (approximately 50% carbon). We assumed that all of the carbon in the fuel was released into the plume during the fire after being converted to the different carbonaceous products of combustion listed above. We further assumed that the concentration of particulate mass remained proportionally constant with reference to the concentrations of the gaseous products of combustion listed above for every Lagrangian parcel in the plume throughout the period of our measurements. This assumption is valid for particles with aerodynamic diameters less than 3.5 μm. The ratio of the mass concentration of carbon in the plume to the mass fraction of carbon in the fuel gives a measure of the mass of fuel required to produce the emissions contained in a unit volume of air in the plume after combustion. The reciprocal of this quantity, when multiplied by the corresponding concentration of particle mass, gives the particle emission factor (EF). This is summarized in the equation:

$$EF = \frac{\overline{P}C_f}{\left(\overline{P}C_p\right) + \left(\overline{CO_2}C_{CO_2}\right) + \left(\overline{THC}\,C_{THC}\right) + \left(\overline{CO}\,C_{CO}\right)} \qquad (1)$$

where $\overline{P}$, $\overline{CO_2}$, $\overline{CO}$, and $\overline{THC}$ are the excess (i.e. above-background) mass concentrations of aerosol particles, CO_2, CO and total hydrocarbons, respectively, and C_f, C_p, C_{CO_2}, C_{CO} and C_{THC} are the fractional masses of carbon in the fuel, smoke particles, CO_2, CO and total hydrocarbons, respectively. The derivation of (1) is given by Radke et al. (1988).

For the current study we assumed a fuel carbon fraction (C_f) of 0.5 (Bryam, 1959; Susott et al., 1991). C_p is measured using programmed ramped temperature heating of quartz filters exposed to smoke, and analysis of the carbon released with the pyrolysis products (Johnson et al., 1981).

As was mentioned in the introduction, Fire A121 was characterized by its low-intensity burning of surface needle fuels with only occasional torching of crowns. Hence, this fire produced CO_2 concentrations that were increased by less than 8% (typically only 5%) over background levels at the sampling altitudes of the aircraft. Given the analytical uncertainty in our CO_2 measurements ($\pm$ 5 ppm approximately), the accurate determination of background CO_2 concentrations was of crucial importance to the computation of reliable emission factors. Therefore, since background concentrations of CO_2 were far more extensively described by the continuous measurements aboard the aircraft than by the two ambient air canister samples (essentially point measurements), we opted to use the continuous measurements of CO_2 made aboard the aircraft in our emission factor computations.

The measured above-background concentration of all carbon-containing products of combustion that were used in the computation of emission factors are listed in Table 2.1. All trace gas concentrations in Table 2.1, except those for CO_2, were measured from the stainless-steel canister samples. CO_2 concentrations were measured in real time from the gases collected in the same 1.5 m^3 bag from which the canisters and filters were filled. Background concentrations of CO_2 were measured immediately prior to entering the plume or immediately subsequent to emerging from it. This was done to eliminate any error in the plume-minus-background CO_2 concentration that might have resulted from the significant drift of the CO_2 instrument. Background concentrations of the gaseous hydrocarbons and CO were taken to be the average of the measurements from two canister samples collected in background air on 28 June 1990. No such samples were collected on 27 June 1990. Several estimates of the background particle mass concentration were derived from the

TABLE 2.1 Above Background Concentrations of all Carbon-Containing Products of Combustion Used in the Computation of Emission Factors

Date	Time (hhmm)	Particle mass conc. (particles <3.5 μm) from 37 mm filters (μg m^{-3})	Particle mass conc. (no size cut) from 37 mm filters (μg m^{-3})	CO_2 (ppm)	CO (ppb)	CH_4 (ppb)
6/27/90	1815	245.7	301.1	17.3	1590.5	125.0
	1856	471.5	524.7	14.3	1185.5	24.0
6/28/90	1513	513.1	587.5	23.6	1195.5	80.0
	1531	399.2	421.3	14.7	1210.5	42.0
	1648	735.5	715.2	28.1	2205.5	151.0
	2041	535.4	574.1	18.7	1451.5	87.0
	2119	532.5	592.3	17.6	1303.5	81.0
	2148	459.6	557.3	18.9	1643.5	100.0

Date	Time (hhmm)	C_2H_6 (ppt)	C_2H_2 (ppt)	C_3H_8 (ppt)	C_3H_6 (ppt)	i-C_4** (ppt)	n-C_4*** (ppt)
6/27/90	1815	21,625.0	4625.0	6500.5	8600.0	275.0	1650.0
	1856	12,875.0	6225.0	2933.5	7567.0	0.0	425.0
6/28/90	1513	6725.0	4525.0	1366.5	4900.0	0.0	100.0
	1531	7075.0	3775.0	1366.5	4433.0	0.0	50.0
	1648	11,675.0	6575.0	3400.5	8133.0	425.0	1475.0
	2041	8875.0	4775.0	1800.5	5133.0	0.0	150.0
	2119	7125.0	4375.0	1333.5	3967.0	0.0	0.0
	2148	9575.0	5075.0	2066.5	5833.0	25.0	225.0

* Background concentrations; an estimate of the background particles mass concentration will be made for the final report.

** Iso-butane (C_4H_{10}); branched-chain paraffin

*** Normal-butane (C_4H_{10}); straight-chain paraffin

particle volume spectra and averaged together to determine a mean background particle mass concentration, which was used for computing emission factors.

3. EMISSION FACTORS FOR SOME TRACE GASES AND PARTICULATE CHEMICAL SPECIES

CO_2 and CO are by far the most abundant carbon-containing products of combustion, with typically over 95% of fuel carbon involved in the production of these two gases (Ward, 1990). Of this amount, CO accounts for approximately 10% [Ward, 1990; the data in Table II and IV in Radke et al. (1991b) suggest a quantity closer to 5%] depending mostly upon the type of combustion (flaming or smoldering) that is occurring. The combustion efficiency (CE) can be defined as the percentage of carbon contained within the fuel prior to combustion that is completely oxidized to CO_2 by the combustion process (Ward, 1990). 100% efficiency, theoretically, is achieved when all of the carbon contained in the fuel is converted to CO_2 following combustion. When the combustion is less than 100% efficient, it is said to be "incomplete" and is characterized by the production of CO and several gaseous and particulate hydrocarbons. It is therefore evident that CO is perhaps the best and most immediate gauge of the inefficiency of combustion, being nearly perfectly anti-correlated with the efficiency of combustion (Ward, 1990, Fig. 9). Hence, much can be inferred about the efficiency of combustion of any given biomass fire simply by examining the quantities of CO and CO_2 produced.

The mean emission factors calculated for several trace gases are listed in Table 3.1. Figures 3.1 and 3.2 graphically compare the mean CO_2 and CO emission factors, respectively, for the Alaskan wildfire with those of two other wildfires ("Myrtle/Fall Creek and "Silver") and several prescribed fires ("Lodi I", "Lodi II", "Hardiman", "Eagle" and "Battersby") examined by Hegg et al. (1990). The lower ratio of the mean CO emission factor to the mean CO_2 emission factor for the Alaskan wildfire compared to those measured for "Mrytle/Fall Creek" and "Silver", both of which burned in southwest Oregon

TABLE 3.1 Average Emission Factors (in Units of Grams Emitted per Kilogram of Fuel Burnt) for Several Trace Gases from the Alaskan Wildfire*

Species	Average Emission Factor
CO	82 ± 12
CO_2	1652 ± 22
CH_4	2.6 ± 1.0
C_2H_6	0.66 ± 0.36
C_2H_2	0.26 ± 0.07
C_3H_8	0.23 ± 0.17
C_3H_6	0.52 ± 0.18
i–C_4	0.0079 ± 0.0138
n–C_4	0.050 ± 0.064
N_2O	0.14 ± 0.08
NO_x **	1.5 ± 0.2
NH_3	0.64 ± 0.31

*For all the species listed in the table (except NH_3) the average emission factors are based on eight samples. The average emission factor for NH_3 is based on five samples. CO_2 and NO_x values are based on continuous measurements, and NH_3 values are based on filter samples. All other values are derived from samples collected in stainless steel canisters.

**$NO_x = NO + NO_2$. Of the NO_x, approximately 85% is NO_2.

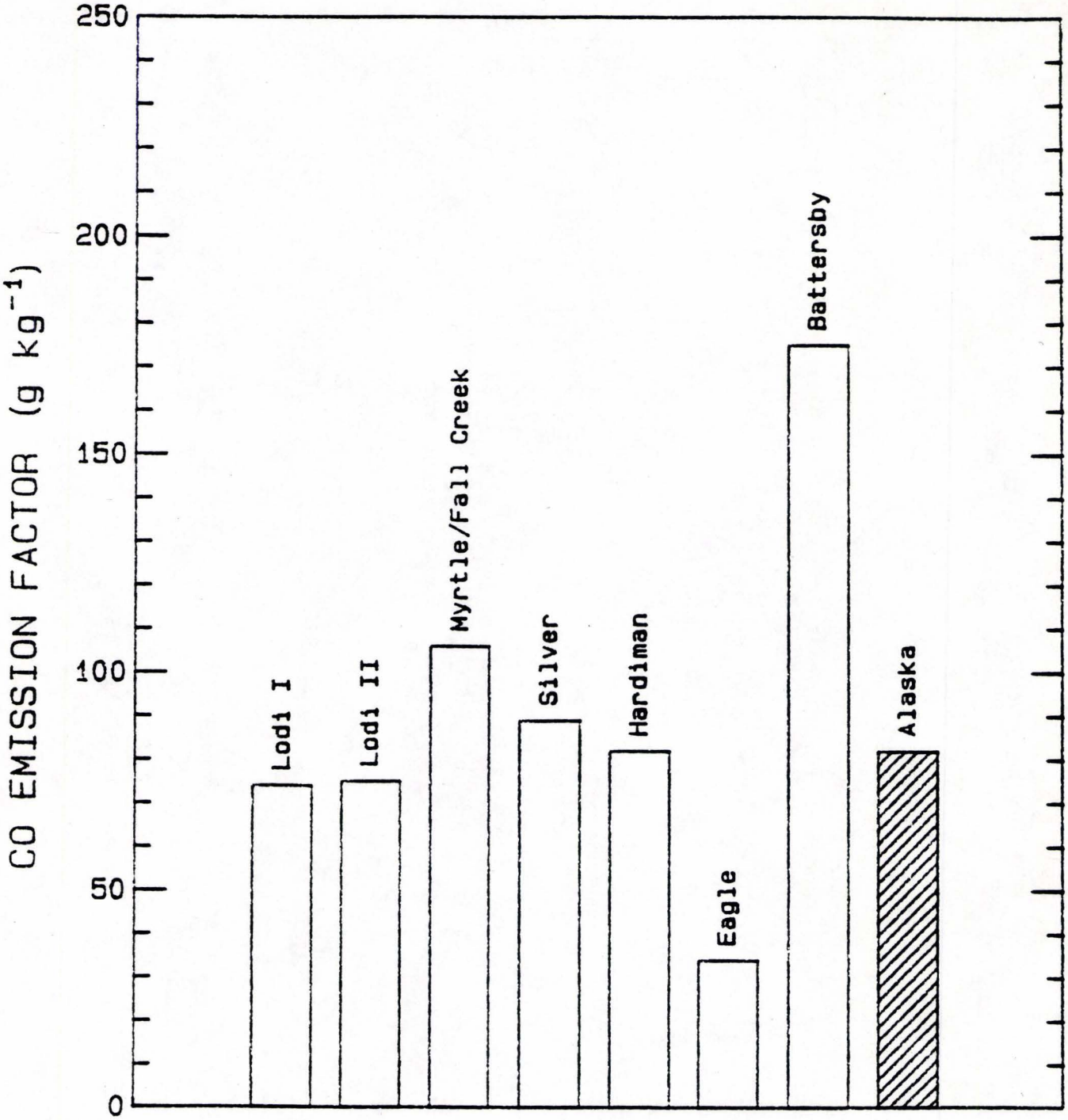

Figure 3.1 Average CO emission factors for the Alaskan wildfire described in this report and for seven fires studied by Hegg et al. (1990).

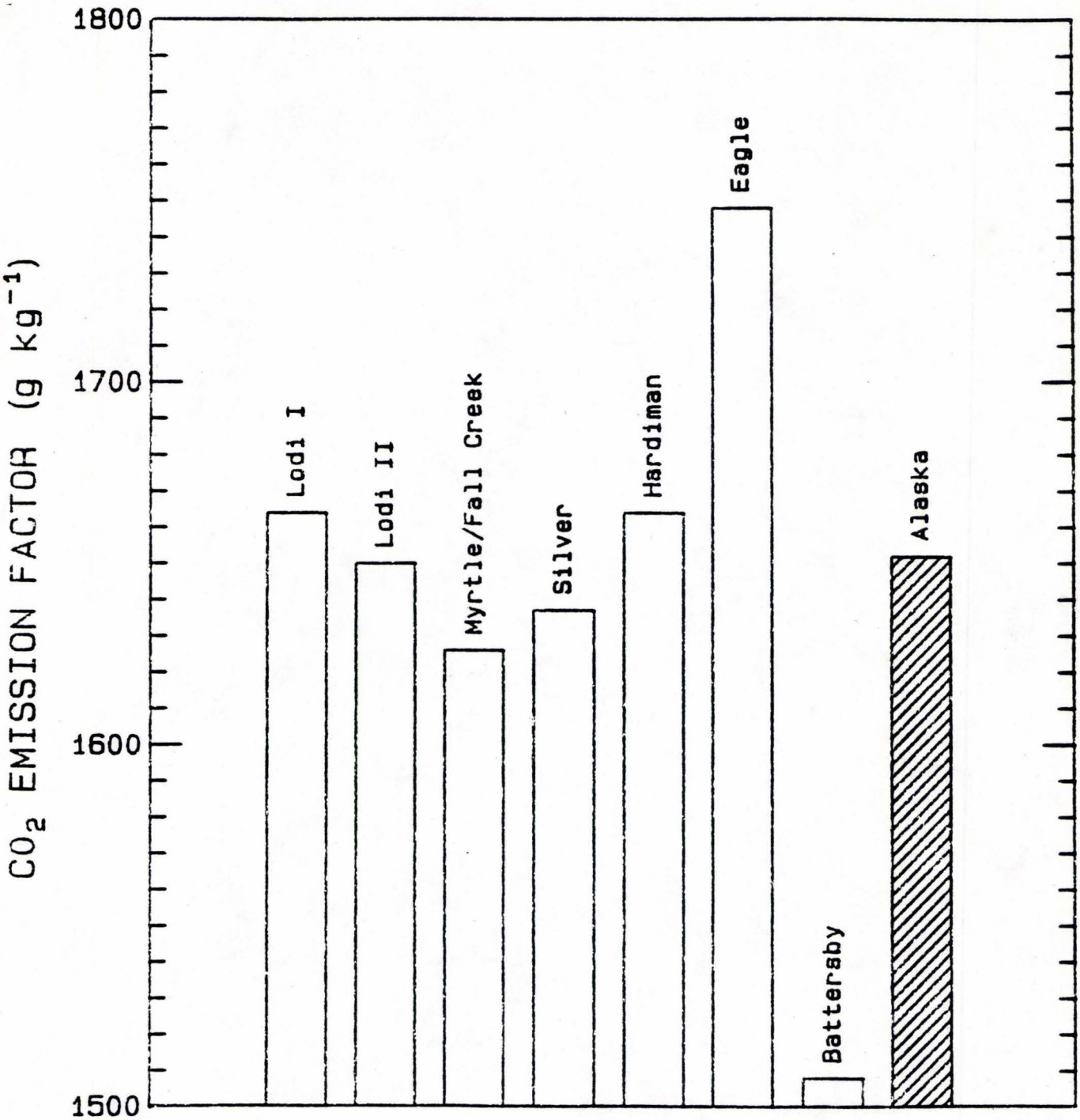

Figure 3.2 Average CO_2 emission factors for the Alaskan wildfire described in this report and for seven fires studied by Hegg et al. (1990).

during the summer of 1987, indicates that the Alaskan wildfire burned with slightly greater efficiency, on average, than the other wildfires during the periods over which they were studied. This may be the result of a more efficient supply of oxygen to the combustion zone at the Alaskan wildfire. Hegg et al. (1990) linked high ratios of CO to CO_2 with high concentrations of H_2, which can only be found in substantial quantities under at least mildly oxygen-limited conditions, and low concentrations of O_2. Thus, under circumstances of oxygen-deficient combustion, we may expect enhanced production of CH_4 and other non-methane hydrocarbons (due to anomalously high levels of H_2), as well as increased production of CO and smoke particles (condensed hydrocarbons) and diminished production of CO_2 (i.e. we may expect less efficient combustion).

From measurements of the emission factors for seven biomass fires, Hegg et al. (1990) calculated a linear regression of the CH_4 emission factor onto the ratio of the CO to CO_2 emission factors and obtained a correlation coefficient (r) of 0.92 significant at >99% confidence level. However, a linear regression of the eight CH_4 emission factors onto the ratios of the CO to CO_2 emission factors for the Alaskan wildfire yields a correlation coefficient of only 0.34. This is not surprising when one considers the internal noise level of the measurements. The uncertainty of the CO_2 measurements alone ($\pm$ 5 ppm) produces a minimum uncertainty of $\pm$ 20%, approximately, in all of our calculated emission factors. This does not include the uncertainty in the measurement of the species in question. An additional factor to consider involves the external conditions under which the fire burned. Unlike many prescribed fires, which burn through distinctive flaming/smoldering life cycles, the Alaskan wildfire burned more uniformly as it advanced through fresh supplies of fuel. This held the combustion efficiency and CO to CO_2 ratios fairly constant. CO to CO_2 ratios computed from the Hegg et al. (1990) data set had a much greater dynamic range compared to those computed from the Alaskan data set (the standard deviations in the CO to CO_2 ratios were 0.03 to 0.008, respectively). The combination of these two effects (uncertainty in the measurements and low dynamic range in the CO to CO_2 ratios) renders a

discernable correlation between ratios of CO to CO_2 and any of the hydrocarbons within the data set from the Alaskan fire unlikely.

A comparison of the mean emission factors from the Alaskan data with those presented by Hegg et al. (1990) gives more meaningful results. For example, the mean CH_4 emission factor listed in Table 3.1 is well predicted by the regression equation obtained from the average emission factors for CO, CO_2, and CH_4 listed in Table 2 of Hegg et al. (1990). When the mean emission factors from Alaska are incorporated into the Hegg et al. (1990) data, a slope of 45.4 and an intercept of 0.3 results from the regression of CH_4 onto CO to CO_2 ratios (Fig. 3.3). The correlation coefficient, $r = 0.92$, is unchanged from the previous analysis (without the Alaska data) and remains significant at a confidence level of > 99%.

An examination of the correlation between total non-methane hydrocarbons (TNMHC), defined here as $C_2H_2 + C_2H_6 + C_3H_6 + C_3H_8 + i\text{-}C_4 + n\text{-}C_4$, and ratios of CO to CO_2 for the Alaskan fire yields slightly better results. A linear regression of the TNMHC emission factor onto the ratio of the CO to CO_2 emission factors produces a correlation coefficient of 0.66 significant at a confidence level of ~90%. With the mean emission factors computed from the Alaska data incorporated into the data from Hegg et al. (1990), an identical analysis gives a slope of 12.1, an intercept of 0.9 and a correlation coefficient of 0.85 significant at a confidence level of >99% (Fig. 3.4). This provides good indication that oxygen-limited, inefficient burning of biomass fuels leads to the production of reduced chemical species.

The average NH_3 emission factor for the Alaskan wildfire was 0.64 ± 0.31 g kg^{-1} (Table 3.1). This lends further support to the finding of Hegg et al. (1990), who measured a mean NH_3 emission factor of 0.9 ± 0.4 g kg^{-1}, that biomass burning is an important global source of NH_3. The NH_3 measured in plumes such as that from the Alaskan fire is generally produced by the pyrolysis of proteins and amino acids in the vegetative tissue.

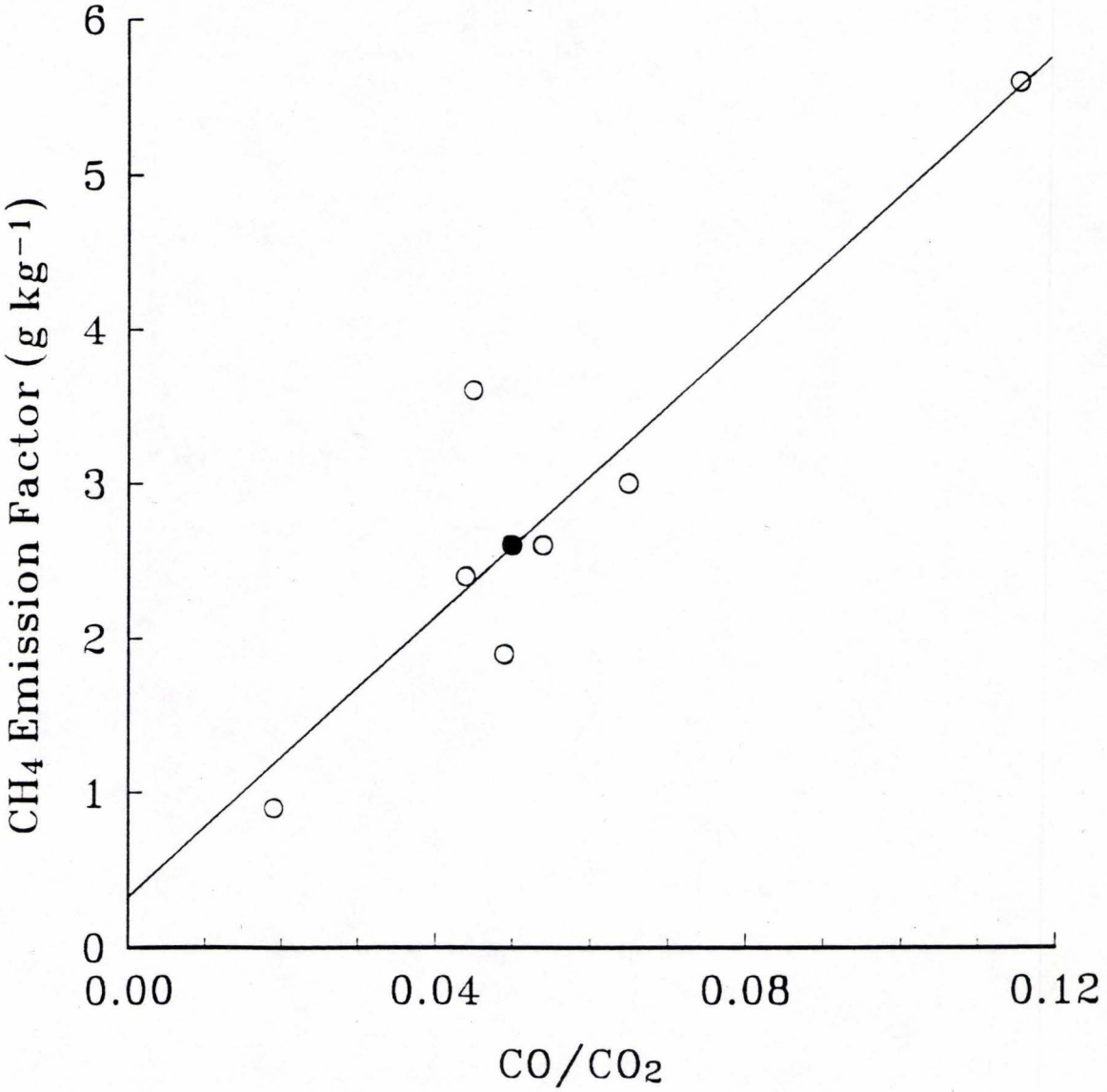

Figure 3.3 Mean emission factor for CH_4 versus the mean ratio of CO to CO_2 emission factors for the Alaskan wildfire (darkened circle) and each of the seven fires studied by Hegg et al. (1990) (empty circles).

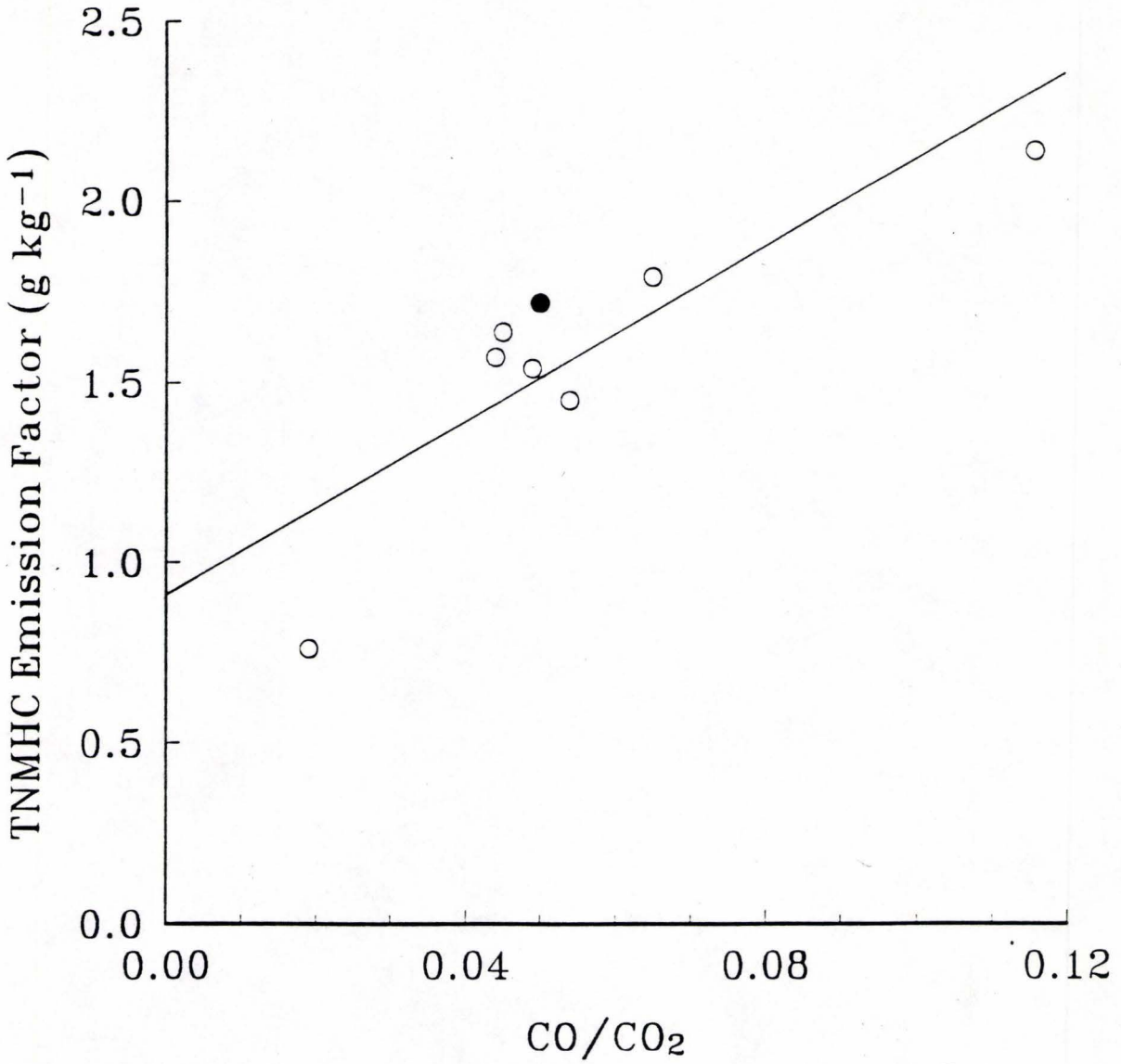

Figure 3.4 Mean emission factor for the total non-methane hydrocarbons (TNMHC) versus the mean ratio of CO to CO_2 emission factors for the Alaskan wildfire (darkened circle) and each of the seven fires studied by Hegg et al. (1990) (empty circles).

There is also some "free" NH_3 in the root nodules of nitrogen fixing plants, but this is unlikely to be a major source.

The extent to which NH_3 is oxidized to odd-nitrogen species (e.g. NO, NO_2, etc.), depends on the availability of O_2 in the combustion zone. Hence, emissions of NH_3 should correlate with the ratio of the CO to CO_2 emission factors. This hypothesis is supported by the data from the Alaskan wildfire. A linear regression of the NH_3 emission factor onto the ratio of CO to CO_2 emission factors yields a correlation coefficient of 0.80 significant at >94% confidence level.

In addition to NH_3, two other gaseous nitrogen species were measured during our study of the Alaskan wildfire: N_2O and NO_x. The average emission factor for N_2O was 0.14 ± 0.08 g kg^{-1}. However, the validity of measurements of N_2O emissions from combustion sources has been questioned recently due to the discovery of an artifact in the use of sampling containers. Muzio and Kramlich (1988) have determined that the storage of moist combustion products containing SO_2 and NO for relatively short periods can produce high concentrations (on the order of several hundred ppm) of N_2O. Even though many of our trace gas measurements are based on samples collected in stainless steel canisters, our N_2O measurements are probably reliable. This is because Muzio and Kramlich found that for SO_2 concentrations below 600 ppm there is negligible production of N_2O, while the typical SO_2 concentrations we have measured in biomass plumes are only ~1–15 ppb. It is also worth noting that the emission factor of 0.14 ± 0.08 g kg^{-1} for N_2O is lower than any of the N_2O emission factors measured by Hegg et al. (1990) in their study of other biomass fires (the smallest average emission factor calculated by these authors was 0.16 g kg^{-1}).

NO_x was the other gaseous nitrogen compound measured in the plume of the Alaskan fire. The average emission factor for NO_x was 1.5 ± 0.2 g kg^{-1} (Table 3.1). This value is slightly lower than the average NO_x emission factor (2.2 ± 1.2) for five of the seven fires studied by Hegg et al. (1990). The two remaining fires ("Lodi 1" and "Eagle")

burned in Southern California and produced much greater quantities of NO_x. Hegg et al. (1990) and Hegg et al. (1987) have suggested that this resulted from the resuspension of pollutants that were previously deposited in the fuel bed.

The mean ratio of NO_2 to NO which we measured in this plume (5.6) was somewhat higher than ratios we have previously measured (2–3; see, for example, Stith et al., 1981 and Hegg et al., 1987). The uncertainty in the NO measurements enables these ratios to be off by as much as a factor of ~2; however, the qualitative predominance of NO_2 in the NO_x emissions is supported by the concurrent O_3 measurements, which indicate that O_3 was reduced from ambient levels only modestly in the bottom part of the plume (i.e. sufficient quantities of O_3 were available for driving the reaction from NO to NO_2). Furthermore, higher ratios of NO_2 to NO in Alaska over those previously measured are implied by the Leighton relationship:

$$k_8[NO_2]/[NO] = k_4[O_3] \qquad (3.1)$$

where $[NO_2]$, $[NO]$ and $[O_3]$ are the concentrations of NO_2, NO and O_3, respectively, k_4 is the rate of the reaction of NO with O_3 to form NO_2 and O_2, and k_8 describes the rate of photolysis of NO_2 to form NO and atomic oxygen (Finlayson-Pitts and Pitts, 1986). Equation (3.1) strictly holds only in air that is void of any organic reactants which include non-methane hydrocarbons. Nevertheless, since k_8 varies proportionally with the radiant flux of ultraviolet light, (3.1) implies that ratios of NO_2 to NO should increase at higher latitudes if O_3 concentrations are held constant. The other fires we studied (Hegg et al., 1990), for which we measured lower ratios of NO_2 to NO and similar concentrations of O_3, burned between 30 and 50 degrees N latitude.

Production of O_3 by the photochemical interaction of reactive hydrocarbons and NO_x in the tops of smoke plumes from biomass fires is well documented (Evans et al., 1976; Stith et al., 1981). O_3 deficits are commonly observed in the bottom parts of smoke plumes. Presumably, this is the result of the loss of O_3 in the reaction with NO, and the decreased efficiency with which NO_2 is photolyzed to subsequently form O_3. An example

of this phenomenon is shown in Figure 3.5. Here, the coefficient of light scattering due to particles (σ_{sp}) is presented to indicate when the aircraft was in the smoke plume. At 1 and 11 minutes, approximately, after the start of this segment of data, during which time the aircraft was flying in the smoke plume at an altitude of 1.2 km, the O_3 instrument registered significant drops in concentration relative to the measurements taken between 4 and 8 minutes when the aircraft was flying outside the smoke plume. At 12–13 minutes, the aircraft climbed 150 m and went back through the plume to find very substantial increases in the concentrations of O_3.

Figure 3.6 shows that O_3 was produced on the sunny side of the plume. This segment of data was collected in the evening (just after 2110 PDT when the sun was low in the sky) in the top part of the plume at an altitude of 1.4 km. During the first four minutes, the aircraft traversed the plume flying directly toward the sun. O_3 levels generally increased, initially, until the aircraft reached the denser inner regions of the plume. Here, O_3 levels began a sharp decline. As the plane emerged from the dense smoke in the central part of the plume and moved into less dense smoke on the sunny side of the plume, a pronounced increase in the concentrations of O_3 was observed. After emerging from the plume entirely, we reversed course (at approximately the 4 minute mark) and flew back through the plume heading away from the sun.

Although O_3 is not emitted directly by fires, it is useful to compute "emission factors" for O_3 which correspond to those computed for NO_x. The data from Alaska produced a mean O_3 "emission factor" of 0.2 ± 0.6 g kg^{-1}. When this data point is added to the Hegg et al. (1990) data set, along with the mean emission factor for NO_x, a regression of the O_3 "emission factor" onto the NO_x emission factor produces a slope of 1.4, an intercept of –2.1, and a correlation coefficient of 0.81 significant at a confidence level of > 99% (Fig 3.7). This suggests that O_3 production is additionally limited by the amount of NO_x available for photolytic reaction with organic compounds in the plume (Hegg et al., 1990).

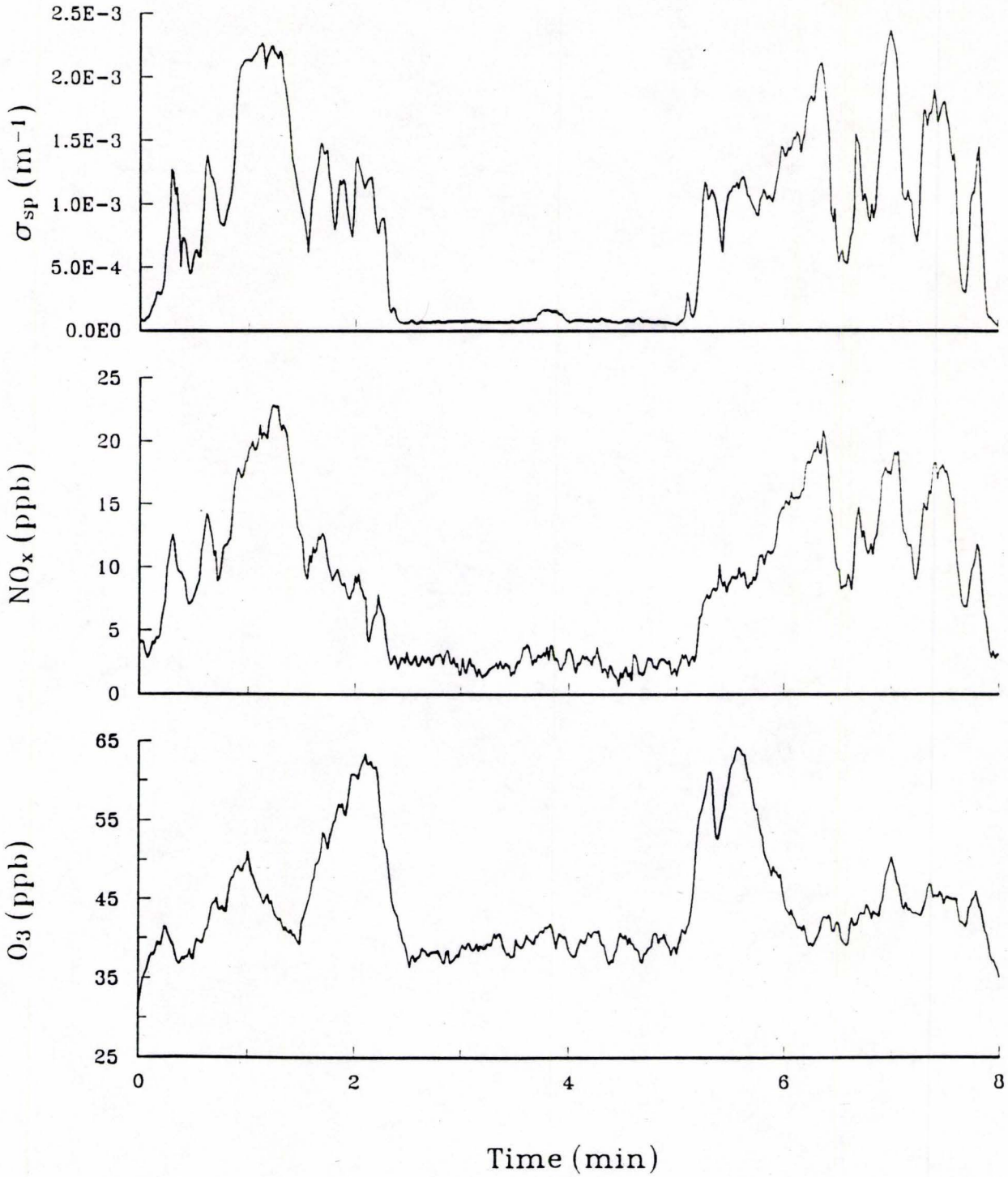

Figure 3.6 Time series of O_3, NO_x and the coefficient of scattering due to particles, σ_{sp}, beginning at 2113 PDT on 28 June, 1990. σ_{sp} is shown to indicate when the aircraft was in plume.

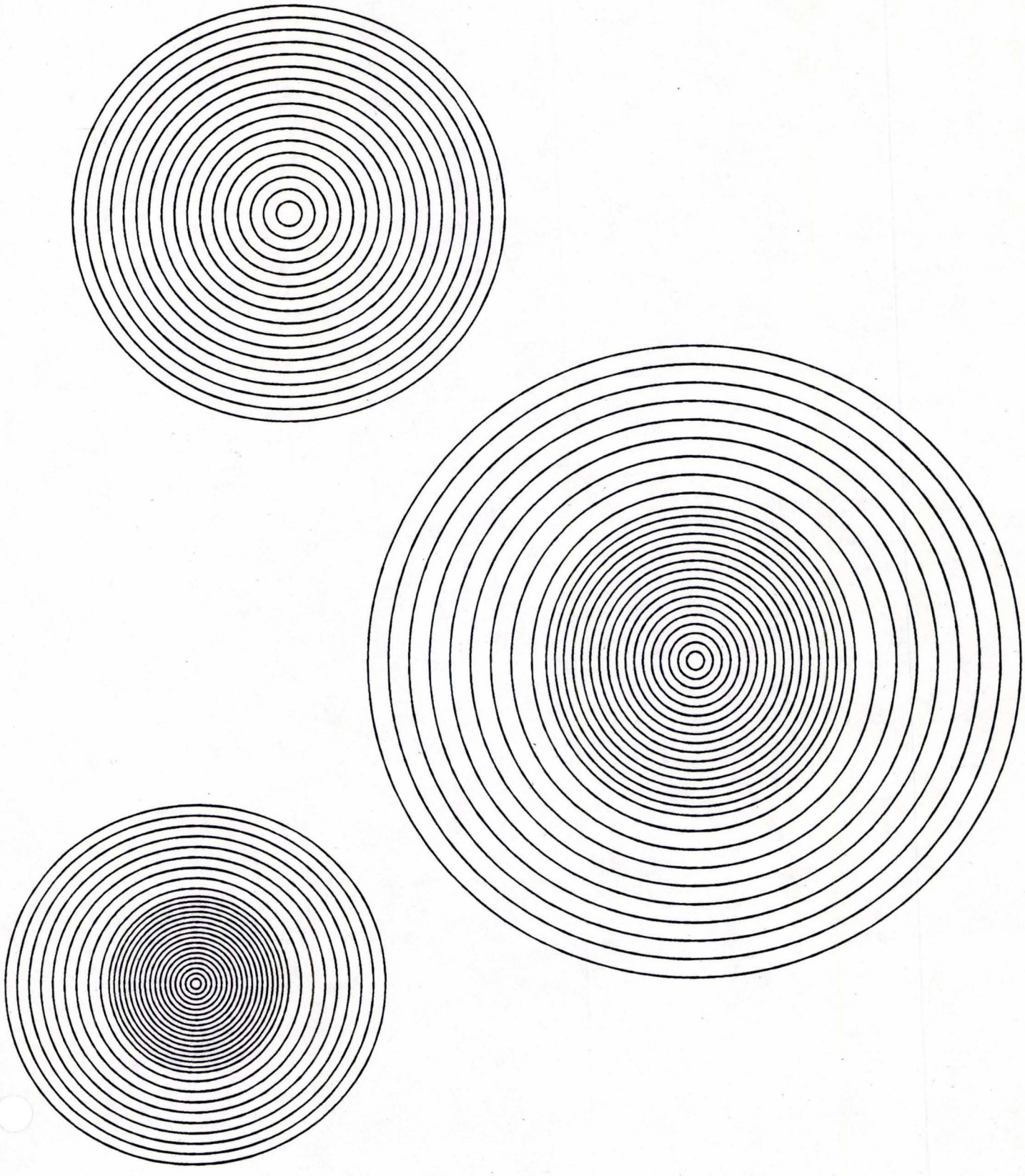

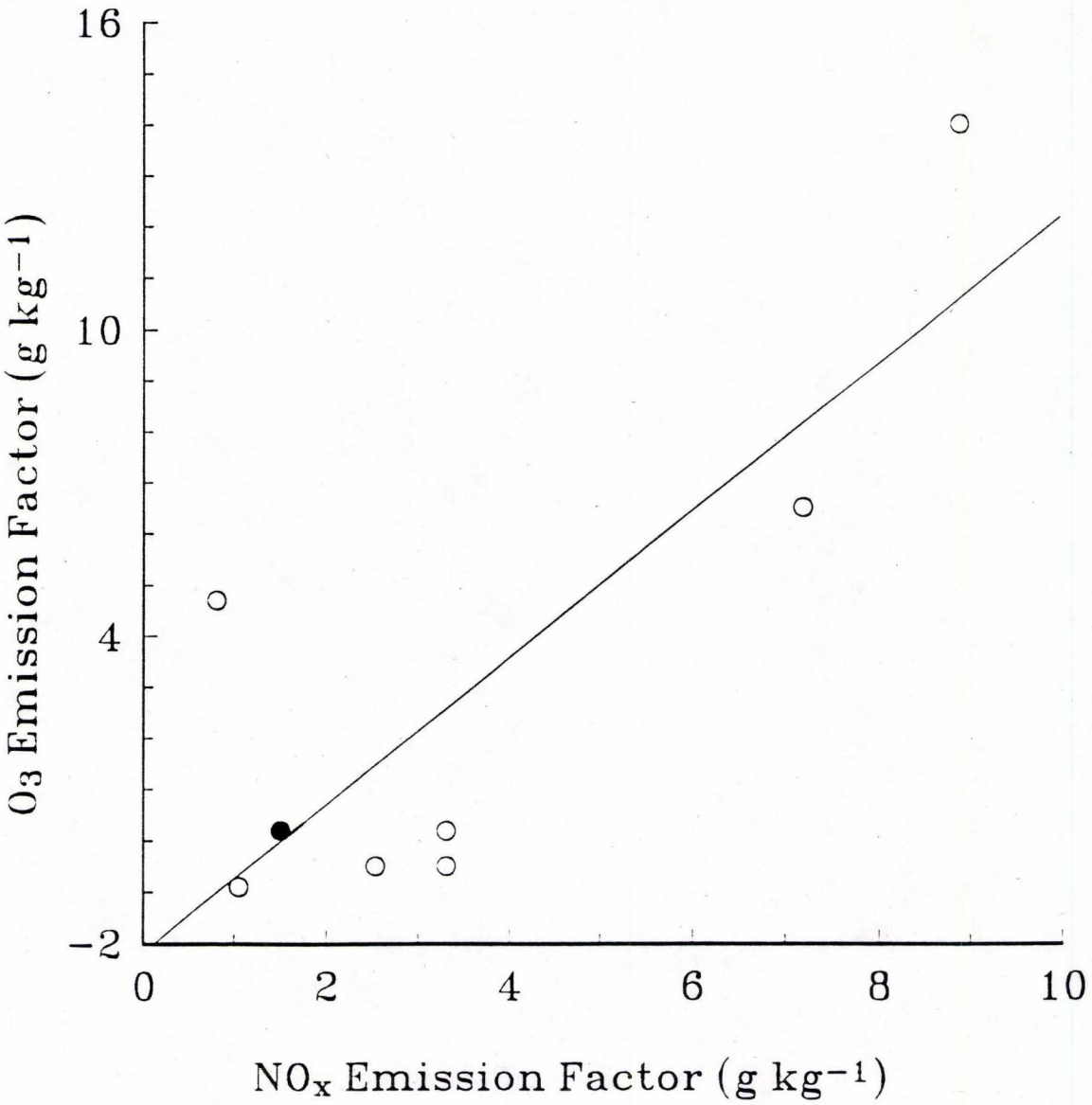

Figure 3.7 Mean "emission factor" for O_3 versus the mean emission factor for NO_x for the Alaskan wildfire (darkened circle) and each of the seven fires studied by Hegg et al. (1990) (empty circles).

The measured concentrations at different locations of various particulate species and gaseous ammonia (NH_3) in the smoke are shown in Table 3.2. All concentrations listed in Table 3.2 were measured from 47 mm filter samples collected on 28 June, 1990.

Measured ratios of sulfate ($SO_4^=$) to nitrate (NO_3^-) emissions ranged from 0.5 to 1.7 with a mean value of 0.86. These ratios are similar to those we measured (average ~0.6) in the smoke from a fire in the San Dimas Experimental Forest in California in 1986 (Hegg et al., 1987) although the concentrations of these two species were about 3–5 times higher in the smoke from the California fire. Hegg et al. (1987) attributed the high $SO_4^=$ and NO_3^- emissions from the San Diego fire to the high deposition of urban pollutants on the vegetation and to their subsequent revolatization during combustion.

Another characteristic of the data in Table 3.2, with possible significance, emerges by looking at the ratios of the concentrations of $SO_4^=$ and NO_3^- to potassium (K^+). K^+ has previously been shown to be a good long-range tracer of aerosol carbon from biomass burning (Andreae et al., 1984). That is, K^+ is essentially inert in a smoke plume, and, once emitted, its concentration can be expected to vary only in response to dilution of the smoke by mixing with environmental air. Thus, by ratioing to K^+, we may learn something about the rates of those reactions that produce $SO_4^=$ and NO_3^- in the smoke plume.

Two samples taken in relatively young smoke near the Alaska wildfire at 2119 and 2148 PDT show that K^+ was emitted in rather substantial amounts from the fire. In a sample of much older smoke (2206 PDT), the concentrations of K^+ were greatly decreased due to dilution (Table 3.2). Conversely, concentrations of $SO_4^=$ and NO_3^- in the older smoke were substantially increased over those measured in the smoke near the fire. Thus, the ratios of both $SO_4^=$ and NO_3^- to K^+ increased as the smoke aged. We attribute this to continuing gas-to-particle conversion of SO_x and NO_x in the smoke plume. At this stage, however, we do not feel justified in trying to estimate the rates of conversion of SO_x and NO_x to $SO_4^=$ and NO_3^- based on ratios of $SO_4^=$ and NO_3^- to K^+ because of the high values of

TABLE 3.2 Concentrations (in μg per m^3 of air) of Various Chemical Species in and Around the Smoke from the Alaska Wildfire. (DL = detection limit of measurements.)

Time (hhmm)	Location	Cl^-	NO_3^-	$SO_4^=$	NH_4^+	Na^+	K^+	$NH_3(g)$
1456	Downwind of capping cumulus cloud	0.53	2.24	3.08	0.57	0.09	0.93	0.29
1513	Near fire	0.97	2.33	3.96	0.32	0.04	1.16	7.93
1531	Near fire	0.58	3.86	2.68	0.43	0.01	0.28	10.17
1551	Upwind of fire	<DL	<DL	0.40	<DL	<DL	<DL	0.32
2041	Near fire	0.85	9.38	4.90	0.28	<DL	0.12	20.13
2119	Near fire	0.98	9.36	5.41	3.46	0.88	4.28	16.68
2135	Upwind	<DL	<DL	0.33	0.30	<DL	<DL	3.96
2148	Near fire	0.82	5.64	3.80	1.95	0.19	1.70	24.84
2206	Old smoke	0.78	13.28	6.57	0.82	<DL	0.41	11.74

these ratios in the sample taken at 2401 PDT in relatively young smoke near the fire (we are not sure why K^+ was not measured in greater quantities in this sample).

The average emission factors for NO_3^-, $SO_4^=$ and ammonium (NH_4^+) are listed in Table 3.3. These averages were computed from a group of 5 measurements listed in Table 3.2 (those taken at 1513, 1531, 2041, 2119 and 2148 PDT) for which we have concurrent measurements from the stainless-steel canisters (Table 2.1). The background concentrations of NH_4^+, NO_3^- and $SO_4^=$ were determined from the upwind samples in Table 3.2.

Only a few studies to date have addressed the production of such species by biomass burning. Andreae et al. (1988) examined emissions of NH_4^+ and $SO_4^=$ from biomass fires in Amazonia, and Hegg et al. (1987) presented data on the production of NO_3^- and $SO_4^=$ from fires near urban areas and in rural locations. The emission factor data for the Alaskan wildfire increases the data available on the emissions of NH_4^+, NO_3^- and $SO_4^=$ from biomass fires and should help to better quantify the source strength of biomass burning for these three species.

4. PARTICLE SIZES AND TOTAL PARTICULATE EMISSION FACTORS

Size Distributions of Smoke Particles

Measurements of the size distributions of smoke particles were made during each of the three flights over the Alaskan wildfire at various distances downwind (1–35 km) of the fire. Our measurements focused on changes in particle size distributions in the smoke as a function of fire behavior, distance downwind (i.e. coagulation time), and cloud scavenging of the smoke particles.

Figure 4.1 compares measurements of average particle size distributions in the smoke plume from the Alaskan fire with those from two wildfires that we studied in Oregon in the summer of 1987. All of the measurements shown in this figure were taken within 5 km of the sources of the wildfires. It can be seen that the number concentrations

TABLE 3.3 Average Emission Factors (in Units of Grams Emitted per Kilogram of Fuel Burnt) for Some Particulate Species from the Alaskan Wildfire

Species	Average Emission Factor*
NH_4^+	0.053 ± 0.066
NO_3^-	0.28 ± 0.15
$SO_4^=$	0.17 ± 0.05

*Values for all three species are based on five filter samples.

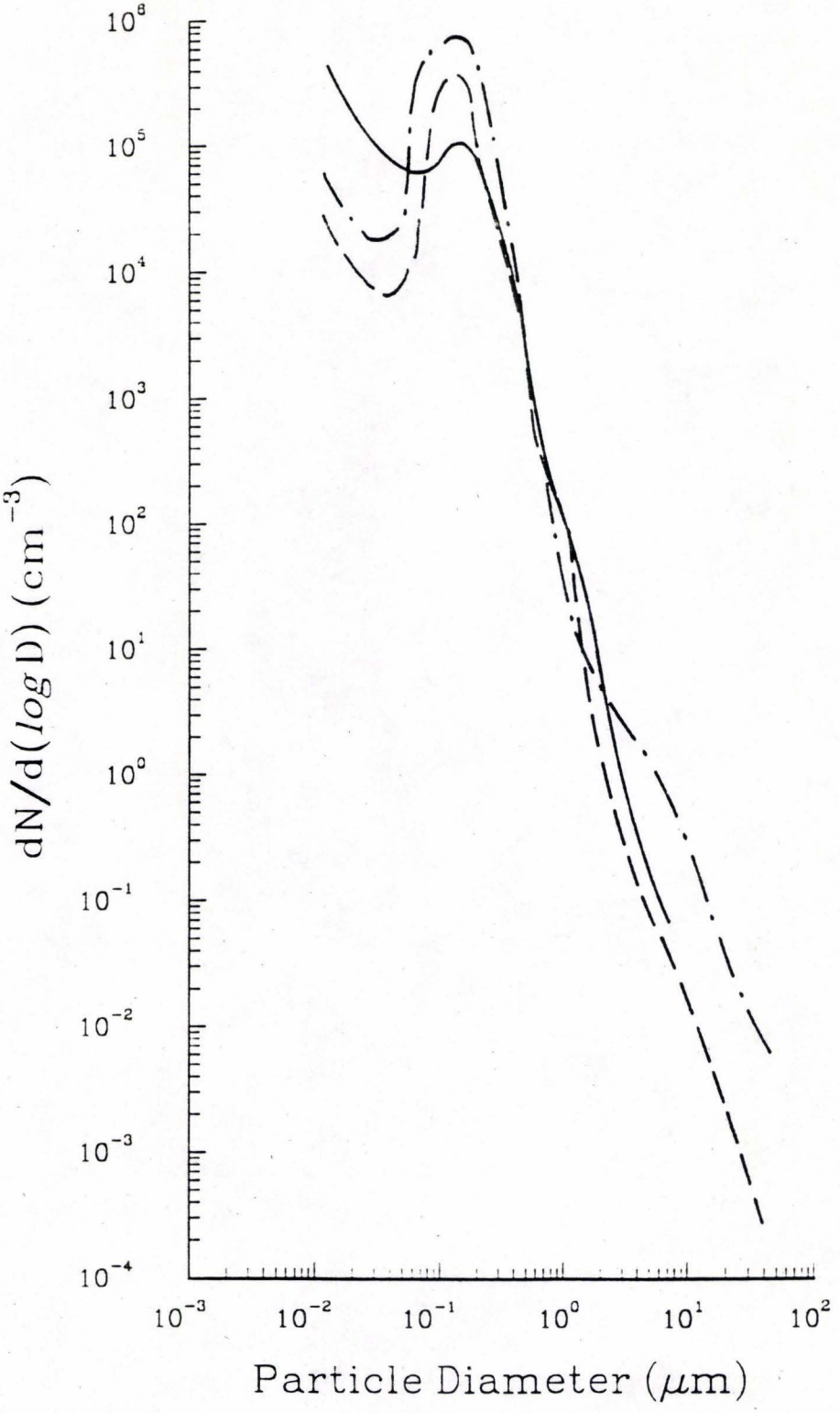

Figure 4.1 Average particle size distributions measured in the smoke close to (<5 km) the sources of three wildfires. The solid line indicates those samples collected at the 1990 Alaskan wildfire. The dashed and dashed/dotted lines represent samples collected at each of two wildfires that burned in Oregon in the summer of 1987.

of particles in the accumulation mode (particles with diameters between 0.1 and 2.0 μm) were much lower for the Alaskan fire than for either of the two Oregon fires. No sample collected in the plume of smoke from the Alaskan fire had a peak accumulation mode number concentration exceeding 2×10^5 cm^{-3}. For particle diameters between 0.5 and 0.9 μm, all three size distributions are essentially identical, and for particles with diameters ≥ 1.0 μm the differences are scarcely significant. Interestingly, in spite of the relatively low number concentrations in the accumulation mode, the smoke from the Alaskan fire had much greater number concentrations in the nucleation mode (i.e. particles with diameters <0.1 μm).

The nucleation mode is often strongly suppressed in forest fire smokes, by rapid coagulation with particles in the accumulation mode. However, when the Alaskan fire was proceeding along distinct, narrow fronts (with little smoldering in the wake of the fire front), dilution reduced the concentration of particles in the accumulation mode to the point that these particles were no longer able to promptly remove particles in the nucleation mode. This interpretation is supported by the data shown in Figures 4.2–4.4, where the measurements are differentiated by the range (time) downwind from the fire. Shown in Fig. 4.2a are average particle size distributions for two smoke samples collected at a mean distance of 3 km and two samples collected at 15 km downwind of the Alaskan fire on 27 June 1990. At 15 km, enough time had elapsed for coagulation to suppress the nucleation mode, even though dilution had reduced the concentration of particles in the accumulation mode to below that at 3 km. This is even more apparent when we contrast the 27 June data with data collected on 28 June at distances of 25–27 km downwind. The particle size distributions at downwind distances of 3 and ~4.5 km (Figures 4.2a and 4.3, respectively) show prominent nucleation modes with particle number concentrations far exceeding those in the accumulation mode. Conversely, the particle size distributions at distances of ~27 and ~25 km (Figures 4.3 and 4.4, respectively) have greatly diminished nucleation modes – most of the particles had evidently coagulated upon accumulation mode particles which

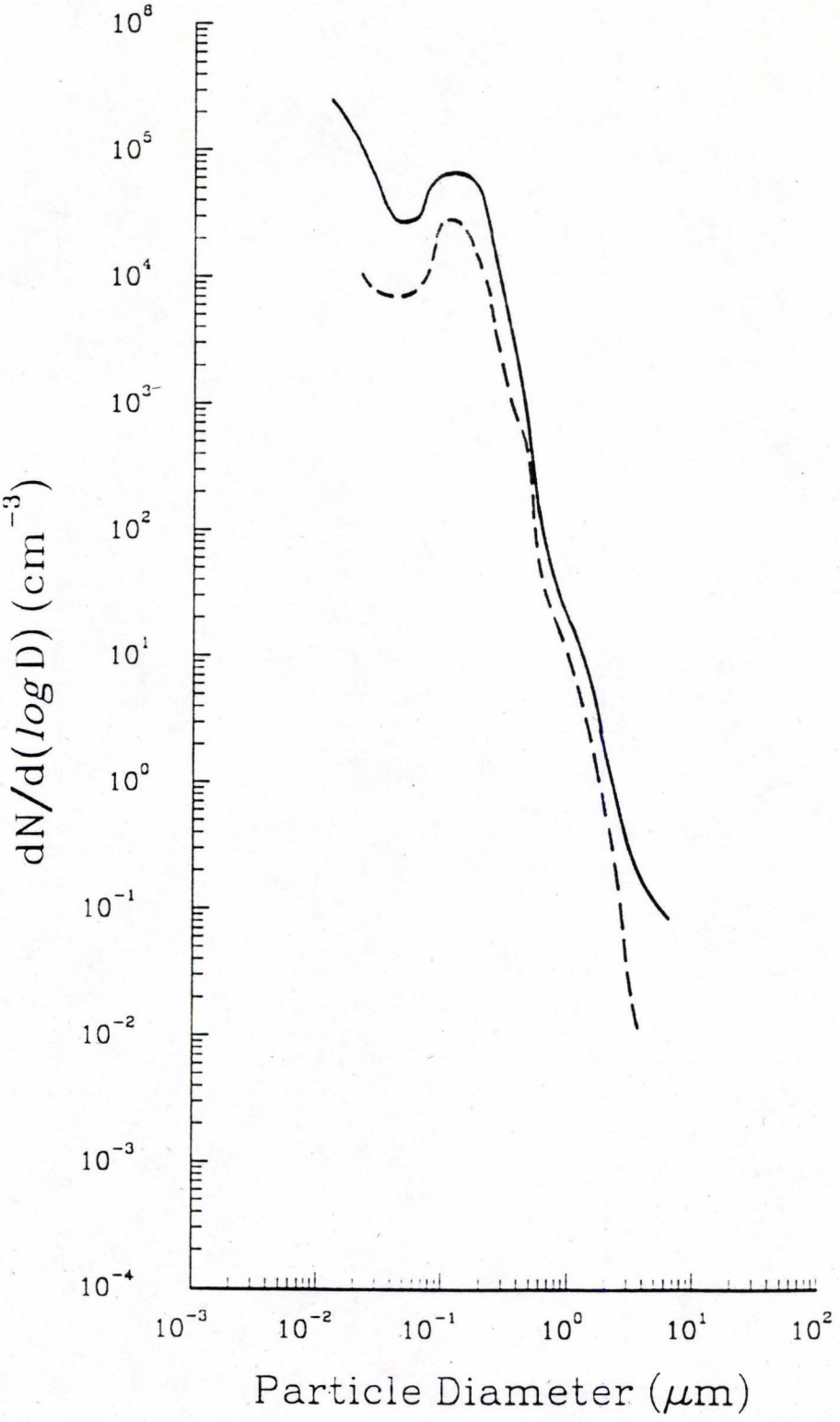

(a)

Figure 4.2 Average number (a) and volume (b) particle size distributions measured in the smoke at a mean downwind distance of 3 km (solid line) and 15 km (dashed line) from the Alaska fire on 27 June, 1990.

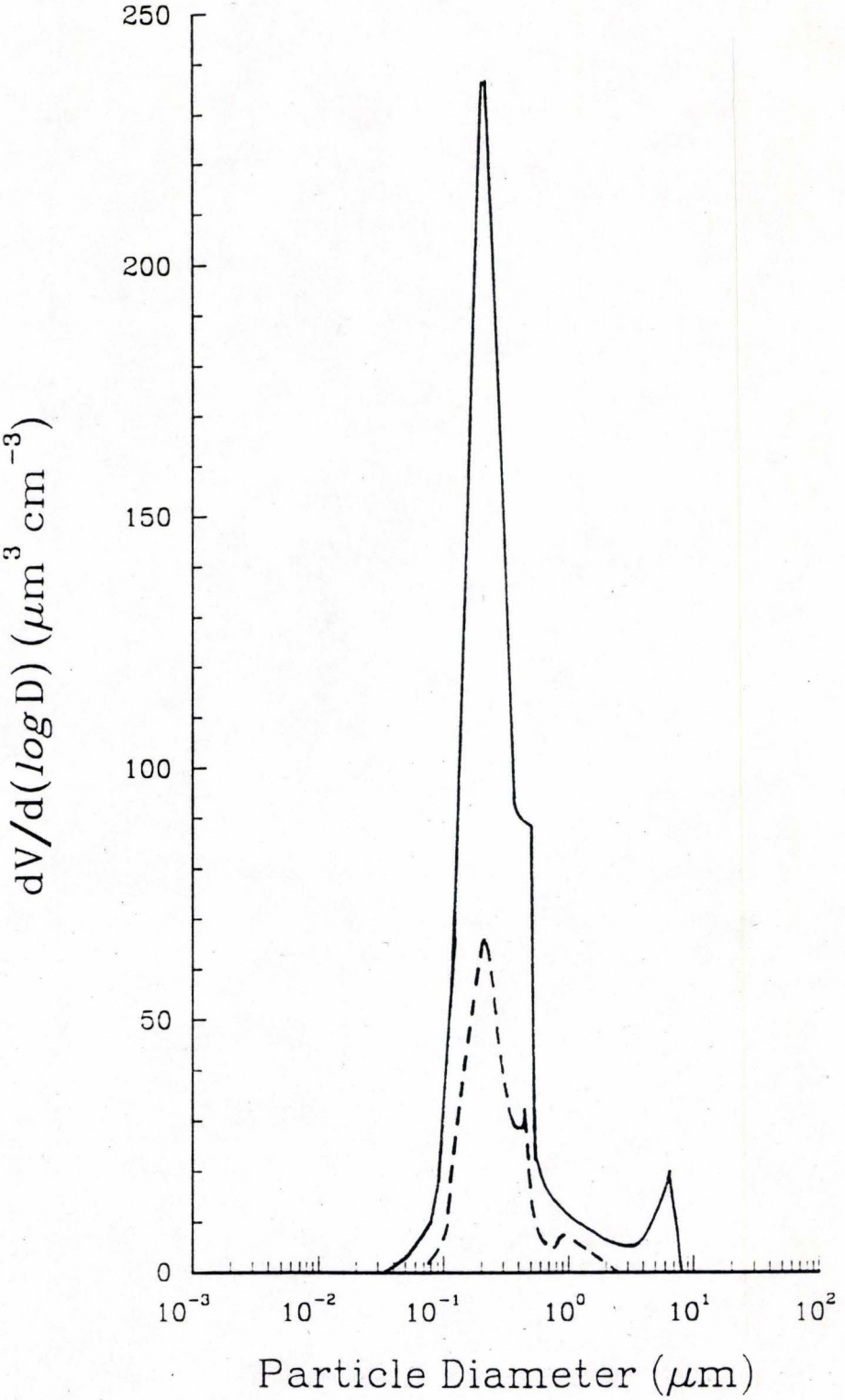

(b)

Figure 4.2 (Continued)

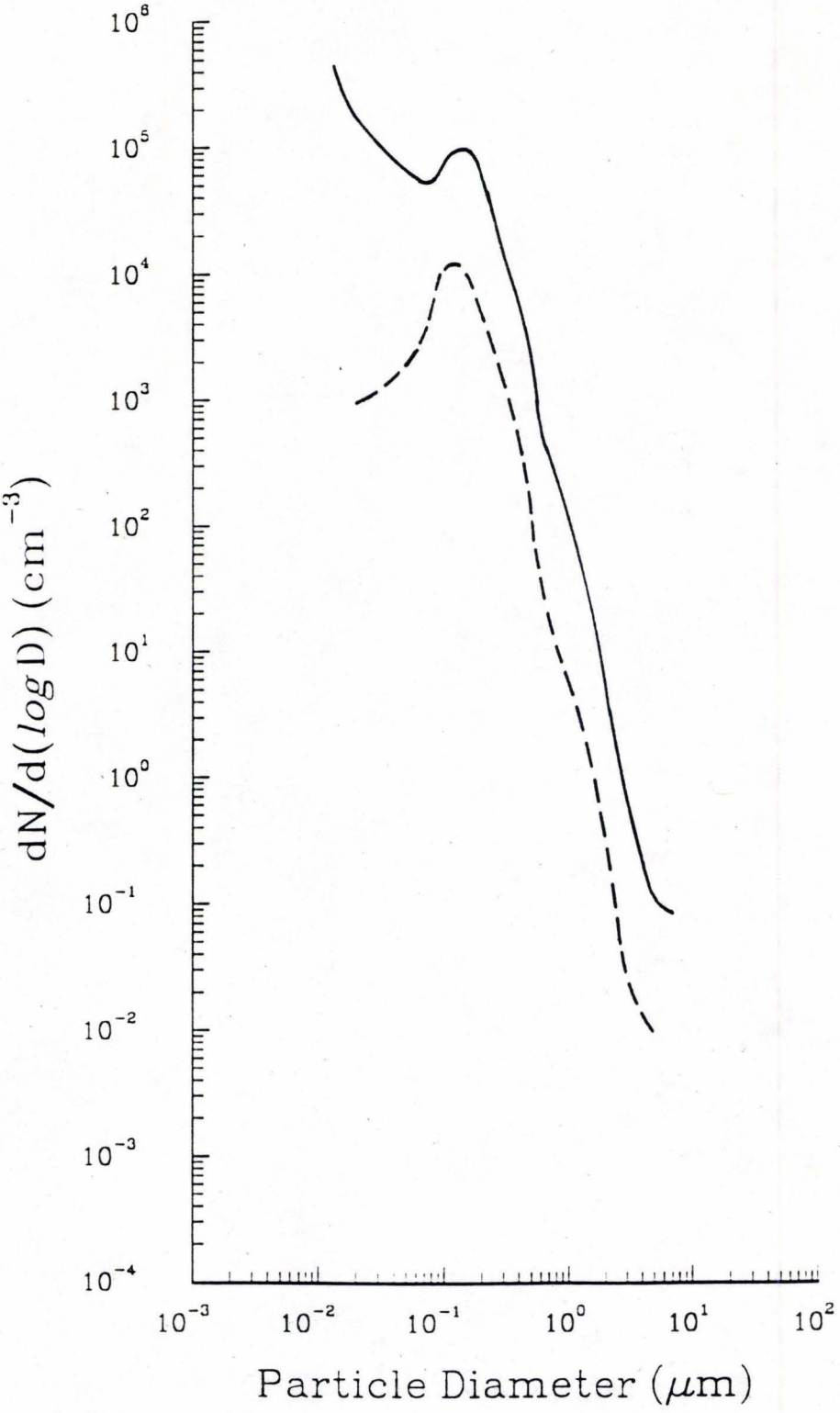

Figure 4.3 Average particle size distributions measured in the smoke from the Alaskan fire on 28 June 1990 at distances from the fire of ~4.5 km (solid line) and ~27 km (dashed line) on 28 June 1990.

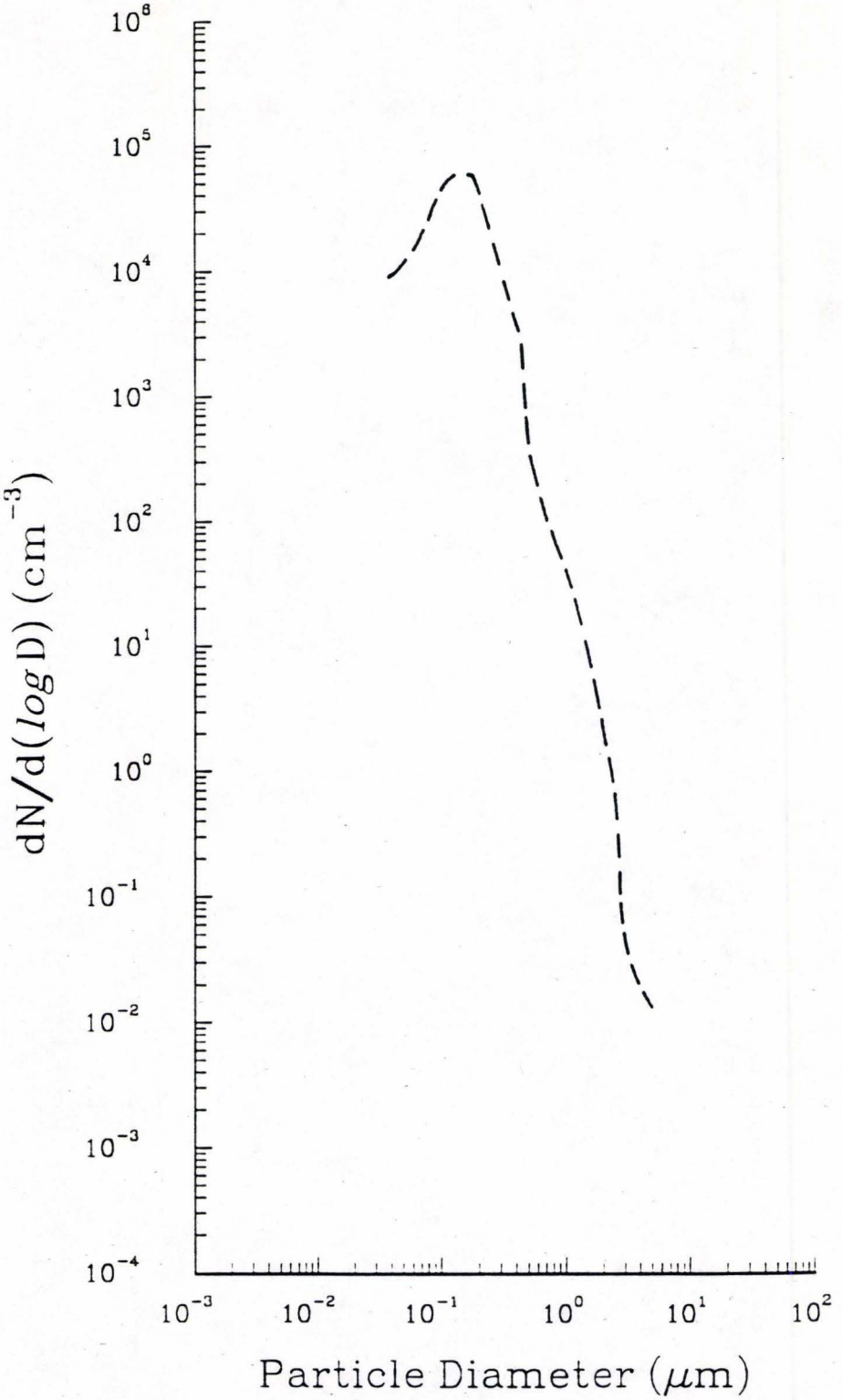

Figure 4.4 Average particle size distributions measured in the smoke from the Alaskan fire on 28 June 1990 at a distance from the fire of ~25 km.

have grown to somewhat larger sizes. The particle size distribution at a downwind distance of ~15 km (Figure 4.2a) has a nucleation mode that is intermediate between those measured farther upwind and farther downwind. Despite this unexpected variation in the nucleation mode aerosol (is this a consistent feature of the smokes from a slowly moving, strongly diluted, linear fire?), these smokes were otherwise rather typical. As can be seen from the particle volume distribution in Figure 4.2b, essentially all of the volume (mass) of the smoke was contained within the accumulation mode, with a modest amount appearing in the coarse particle mode (>2 μm) close to the fire. This means that the optical properties, and therefore visual blight of the smoke, were dominated by the particles in the accumulation mode. This feature is one of the constants observed in all of our biomass fire studies to date (Radke et al., 1991b). Since the accumulation mode is very resistant to atmospheric removal by any process other than cloud scavenging, it continues to be evident why biomass smokes are so often persistent in the atmosphere.

Total Particulate Emission Factors

Computation of particulate emission factors from the 37 mm Teflon filter measurements yielded mean values of 21.3 ± 4.3 and 23.9 ± 4.9 g kg^{-1} for fine particles (d < 3.5 μm) and "total" particles, respectively. Ward and Hardy (1991) derived regression equations, based on data collected within about 10 m of the ground, that predict the particle emission factor from the measured combustion efficiency:

$$EFPM = 93.3 - 90.5\ (CE) \qquad (4.1)$$

$$EFPM_{2.5} = 67.4 - 66.8\ (CE) \qquad (4.2)$$

where, EFPM is the emission factor for particle mass, $EFPM_{2.5}$ the emission factor for particles < 2.5 μm in diameter, and CE the measured combustion efficiency. They further derived the equation EFPM = 108.6 – 108.0 (CE) from the ground-based data in Fig. 5 of Hegg et al. (1990). Since the mean combustion efficiency measured at the Alaskan fire was approximately 91%, these equations suggest that the mean emission factors we

computed from the data collected in Alaska are about 2–3 times too high. This raises the possibility that our measurements of particle mass concentrations are in error. However, our measurements of the specific scattering, B_S, of the smoke particles ($B_S = \sigma_S/\rho$ where ρ is the mass concentration of particles) gives a mean of 2.9 ± 0.5 m^2 g^{-1}. This is very similar to values of B_S reported by other investigators (e.g. Patterson and McMahon, 1984 and Tangren, 1982). Since B_S should vary only in response to significant changes in the size distribution of particles, this indicates that our measured particle mass concentrations are reliable.

Equation (4.2) implies that a particle emission factor of 20 g kg^{-1} would require a combustion efficiency of ~70%. This is lower than we have ever observed in our airborne studies of biomass fires. The mean combustion efficiency measured for the "Battersby" fire, the least efficient of all the fires studied from an airborne platform by Hegg et al. (1990) and Radke et al. (1991b), was about 85% (based on mean measurements of CO and CO_2). This reflects the integrated nature of smoke plumes at high altitudes. Measurements made with ground-based instrument systems are much more effective at identifying smoke from distinctive combustion phases (with distinctive combustion efficiency characteristics; see Ward, 1990), while, at higher altitudes, the plume becomes a more homogeneous blend of smoke from all phases of combustion. The mean combustion efficiency for all of the fires studied by Radke et al. (1991b), based on the mean emission factors for CO and CO_2 from each fire, was approximately 92%. When this figure is substituted in (4.2), a mean $PM_{2.5}$ emission factor of ~6 g kg^{-1} is predicted. The mean $PM_{2.5}$ emission factor reported by Radke et al. (1991b) is 15 g kg^{-1} (the contribution of particles between 2.5 and 3.5 μm in diameter is insignificant). This suggests that gas-to-particle conversion at altitudes greater than 10 m above the surface (approximately the altitude at which smoke particles were sampled by Ward and Hardy (1991) may be quite substantial.

5. OPTICAL PROPERTIES OF THE SMOKE

The optical properties of biomass smoke are of particular interest and importance, yet the amount of data that is available on the optical properties of wildfire smokes is extremely limited.

Measurements of σ_e and σ_s for a typical transect of the plume from the Alaskan wildfire are shown in Figure 5.1. The lower curve shows the measurements for σ_s and the upper curve the measurements for σ_e. σ_a can be inferred from the difference between the two curves. A single numerical value for $\tilde{\omega}$ is printed within the frame of Figure 5.1. This is the computed average value for $\tilde{\omega}$ across the entire plume. The measurements shown in Figure 5.1 were taken within 5 km downwind of the fire.

The optical properties of smoke particles from biomass burning can be highly variable, since they depend on a number of factors, including the type of fuel burned, the intensity of the fire, and the phase of combustion (McMahon, 1983; Patterson and McMahon, 1984). During the early, flaming phase of combustion, the conditions support pyrolytic production of particles consisting of high concentrations of both single spheres and sooty chains that are optically very absorbing. In the later, smoldering phase of combustion, the smoke is dominated by weakly or non-absorbing liquid (waxy) and solid particles, consisting of organic materials (with a range of volatility) and non-sooty inorganic materials. Patterson and McMahon (1984) found that as a fire changed from the flaming phase into the smoldering phase of combustion, particle emissions increased while the specific absorption ($B_a = \sigma_a/\rho$, where ρ is the mass concentration of smoke particles) decreased. However, their measurements were made on smokes produced in a laboratory, where burning conditions were strictly, but not necessarily realistically, controlled. In the field, smokes often consist of mixtures of particles from various stages of combustion. Nevertheless, some of our studies of prescribed burns of forest slash show trends in particle emissions, and in the optical characteristics of the particles, with changes in the phase of combustion (see Radke et al., 1991b).

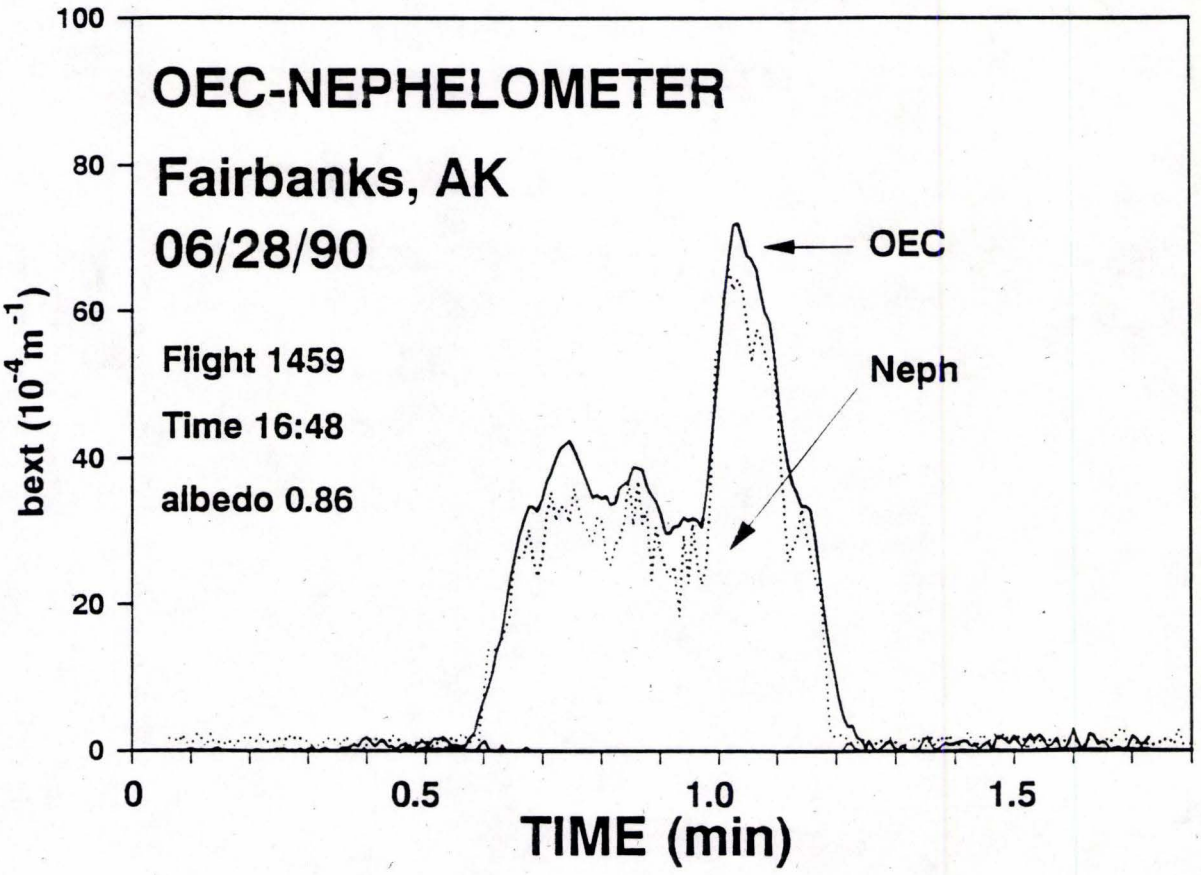

Figure 5.1 Measurements of the light-extinction coefficient (σ_e) and light-scattering coefficients (σ_S) made during a transect of the smoke plume from the Alaskan wildfire at a distance of ~3 km from the source of the fire on 28 June 1990. The difference between the two curves gives the light absorption coefficient due to the particles (σ_a).

As we have previously mentioned, prescribed fires differ from wildfires in that they can be rapidly ignited and subsequently allowed to burn out. This can lead to flaming and smoldering phases that are easily distinguishable, which is a necessary condition for distinct trends in the optical and emissions properties of the smoke. Some of the measurements that we have obtained in the smoke from prescribed fires show a correlation between the emission factor for fine particles and $\tilde{\omega}$, both of which tend to increase as a fire progresses through the flaming phase and into the smoldering phase. Not surprisingly, no such correlation was observed in the data from the Alaskan wildfire. The mean value of thirteen different measurements of $\tilde{\omega}$ taken in the smoke from the Alaskan fire was 0.82 with a standard deviation of only 0.02. The range of the $\tilde{\omega}$ measurements was 0.78 to 0.86 (is this surprising uniformity of $\tilde{\omega}$ characteristic of boreal wildfires?). This narrow range suggests, as expected, that the smoke was a fairly uniform mixture of particles from various stages of combustion. In a prescribed fire that we studied in British Columbia, we measured values for $\tilde{\omega}$ that ranged from 0.48 early in the flaming phase of combustion to 0.94 later in the smoldering phase of combustion (see Radke et al., 1991b). The mean of all transect-averaged values of $\tilde{\omega}$ that were measured during the Alaskan fire (0.82) is typical of other prescribed biomass fires and wildfires as well [Radke et al. (1991b) give an average value for $\tilde{\omega}$ of 0.83 for a group of seventeen prescribed biomass fires and wildfires].

Measurements of B_a were obtained from the 37 mm Teflon filters from which σ_a was measured using the integrating plate method (Weiss et al., 1979), and the mass concentration of particles was measured as previously described. The measurements from 13 filters produced a mean value of 0.75 ± 0.23 m^2 g^{-1}. This compares with a value of 0.64 m^2 g^{-1} for all 17 fires studies by Radke et al. (1991b). Patterson and McMahon (1984) measured values ranging from ~1m^2 g^{-1}, for the flaming combustion phase, to ~0.04 m^2 g^{-1} for the smoldering combustion phase. Thus, a mean value of 0.75 m^2 g^{-1} implies a mixture of smoke particles from all combustion phases (flaming, smoldering, and

transitional) with perhaps the dominant component being supplied by the flaming combustion phase.

6. SHAPES OF THE SMOKE PARTICLES

The particle size characteristics of the smokes from biomass fires suggest that they will have rather long residence times in the atmosphere, which increases their potential for adverse environmental effects. This is because most of the particle mass resides in the accumulation mode (0.1 – 2.0 μm diameter), where sedimentation velocities are negligible and coagulation rates are rather slow (Fuchs, 1964; Radke et al., 1991a). The only known efficient removal mechanism for accumulation mode particles is cloud scavenging (Radke et al., 1991a), which can be effective because a large fraction of the smoke particles can serve as cloud condensation nuclei.

The actual atmospheric residence times of biomass smokes remains uncertain. One of the largest uncertainties involves how the residence time is affected by coagulation. Unlike smokes from hydrocarbon fuels, which consist largely of chain aggregates (Radke et al., 1990), fresh biomass smokes consist largely of single spheres in the accumulation mode (Radke et al., 1988; Cofer et al., 1988). These spheres are formed by condensation near the combustion zone and grow rapidly as the emitted heavy organic vapors cool. Initially, these particles are best described as oily or waxy; evidence of early coagulation may be masked by particle coalescence, although the details remain elusive (Wornat and Sarofim, 1990). Rodgers et al. (1990) and Radke et al. (1991a) obtained evidence of enhanced coagulation and the formation of chain aggregates in dense biomass smokes that were at least 24 hours old. We have not examined particle morphology at intermediate ages.

Because of the paucity of data on the affects of aging on particle shapes (which affect coagulation and sedimentation velocities in biomass smokes) we have built a new instrument to obtain quantitative data on the asymmetry in the shapes of atmospheric

aerosol particles. This instrument, called the Aerosol Asymmetry Analyzer (A^3), is based on the work of our Soviet colleague Dr. V. N. Kapustin. The A^3 consists of a cell, ~ 0.3 m in length and 1 cm high, that forms a parallel plate capacitor (Figure 6 .1). A polarized He-Ne laser beam is introduced at one end and the light scattering coefficient is measured using the geometry of an inverse nephelometer (Gerber, 1979). A high voltage (2000 V dc) is applied to the capacitor for 10 ms and then switched in polarity (~1 μs). After 10 ms with opposite polarity, the high voltage is turned off for 80 ms. When smoke is introduced into the cell, the induced or permanent dipole on the particle causes it to orient in the electric field. If all the particles are spheres, no change in scattering will occur when the field is applied. If, on the other hand, some of the particles are asymmetrical, the change from random orientations to an ordered orientation in the presence of the applied field will cause a pronounced increase in light scattering. The ratio of the light scattering coefficient from the random to ordered orientation is called the "asymmetry ratio", which is proportional to the length-to-width ratio for simple asymmetrical particles (such as single or primary chain aggregates).

If the particles have a permanent dipole, they "flip" when the electric polarity is reversed, while if the dipoles are induced by the applied field there is no flipping. The time needed to "relax" to a random orientation with the voltage off is a measure of the particle size.

Our airborne measurements in the Alaskan wildfire provided the first opportunity to use the A^3 aboard our aircraft. Particles in the "young" smoke (~0.5 hours old) from these fires was identified by the A^3 as symmetrical (i.e. spherical), which confirms our tentative earlier work in which we used electron microscopy to study smoke particles. As the smoke aged to about 3 hours, it remained symmetrical. As noted in Section 4.1, there is some hint that the mean size of the particles in the accumulation mode increased modestly over the first 3 hours. If coagulation were responsible for this change, the A^3 results suggest that,

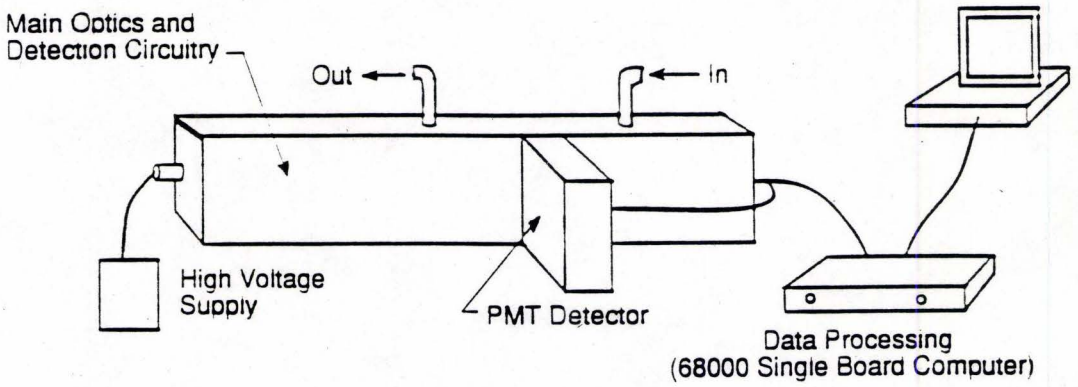

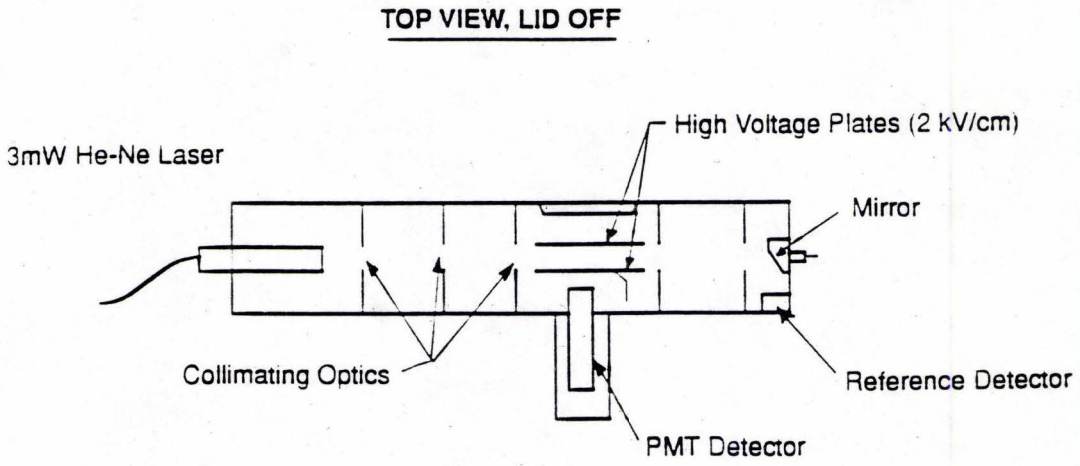

Figure 6.1 Schematic of the Aerosol Asymmetry Analyzer.

at least over the first 3 hours, the smoke particles were sufficiently liquid at their surfaces to mask any evidence of collisions.

Since spheres have the highest fall speed for a given mass, early coalescence of aggregates works to reduce the atmospheric residence time of biomass smokes. A priority in our next set of measurements will be to use the A^3 instrument to investigate the shapes of dense smokes with ages between 3 and 24 hours.

7. SCAVENGING OF THE SMOKE BY CLOUDS

We have found previously that biomass smokes can be scavenged rather efficiently by clouds (Radke et al., 1991b). In the Alaskan wildfire, we had the opportunity to observe some interactions between the smoke and the modest sized cumulus clouds that capped the fire.

Referring back to Table 3.2, the sample collected in the smoke plume downwind of the modest fire-capping cumulus cloud (at 1456 PDT) shows that NH_3 was rather efficiently scavenged from the plume by the cloud, resulting in concentrations of NH_3 that were actually slightly lower than in the smoke-free air upwind of the fire. On the other hand, particulate NH_4^+ was higher in the sample collected downwind of the capping cumulus than in the two samples collected upwind of the cloud at 1513 and 1551 PDT. The molar ratio of NH_4^+ to $SO_4^=$ was 0.99 in the cloud-processed smoke, while in the unprocessed smoke the ratios were 0.43 and 0.86. This suggests that gaseous ammonia was efficiently taken up by acidic cloud droplets, leaving behind more ammoniated, but still acidic, sulfate aerosols after evaporation.

8. SUMMARY

The Alaskan wildfire described in this report appears to have burned with typical efficiency compared to several other North American wildfires and prescribed fires we have studied in the mid-latitudes (Hegg et al., 1990; Radke et al., 1991b). Internally, we found

signs of significant correlation between ratios of CO to CO_2 emission factors (related to combustion efficiency and proportionally linked to oxygen deficient combustion) and emissions of a subset of non-methane hydrocarbons and NH_3. O_3 was qualitatively found to be strongly dependent on the radiant flux of ultraviolet light as expected. The mean emission factors computed from the data collected in Alaska are easily integrated into the data set published in Hegg et al. (1990) and lend further support to their conclusions that 1) CH_4 emissions vary proportionally with ratios of CO to CO_2 emissions, 2) O_3 production in smoke plumes is limited by the amount of NO_x available for reaction with organic compounds, and 3) biomass fires are a major global source of atmospheric NH_3.

The mean emission factor for particles < 3.5 μm was 21.3 ± 4.3 g kg^{-1}. Radke et al. (1991b) found a mean of 15.0 g kg^{-1} in an airborne study of several fires. Given the average combustion efficiency of these fires (~92%), the results of the ground-based study of Ward and Hardy (1991) predict much lower values (~6 g kg^{-1}). This suggests there is substantial gas-to-particle conversion above the ~10 m sampling altitude used in their study.

The small variability in our measurements of the single scattering albedo of the smoke (0.82 ± 0.02) reflects the lack of a progression of this wildfire through the distinctive combustion phases that are often present in prescribed fires. In combination with the mean value of B_a (0.75 ± 0.23 m^2 kg^{-1}), this suggests a uniform blend of smoke from all combustion phases with a primary component from the flaming phase.

Measurements of particle size distributions in the Alaskan wildfire show a nucleation mode that is relatively strong and persistent. We have suggested that this is the result of a low coagulation rate due to the relatively low number concentrations of smoke particles in the accumulation mode. The low number concentrations of accumulation mode particles seems to have been due to rapid mixing and dilution of smoke with the ambient air as a result of the linear manner in which the fire advanced.

Measurements of gaseous NH_3 in smoke processed by a water cloud suggest that it is efficiently scavenged by clouds. Also, our measurements of particulate NH_4^+ and $SO_4^=$ suggest that cloud processes may help to partially neutralize sulfate aerosols that are left when the cloud droplets evaporate.

Finally, data collected with a new airborne instrument suggest that for aging times up to ~3 hours the particles in the smoke from the Alaskan wildfire were mainly spherical. This has important implications for the residence times in the atmosphere of such smokes.

9. REFERENCES

Andreae, M. O., T. W. Andreae, R. J. Ferek and H. Raemdonck, 1984: Long-range transport of soot carbon in the marine atmosphere. The Science of the Total Environment, 36, 73–80.

Andreae, M. O., E. V. Browell, M. Garstang, G. L. Gregory, R. C. Harriss, G. F. Hill, D. J. Jacob, M. C. Pereira, G. W. Sachse, A. W. Setzer, P. L. Silva Dias, R. W. Talbot, A. L. Torres and S. C. Wofsy, 1988: Biomass-burning emissions and associated haze layers over Amazonia. J. Geophys. Res., 93, 1509–1527.

Bryam, G. M., 1959: Combustion of Forest Fuels. In Forest Fire Control and Use, edited by K. P. Davis, McGraw–Hill, New York, NY, 321 pp.

Cofer, III, W. R., J. S. Levine, D. I. Sebacher, E. L. Winstead, P. J. Riggan, J. A. Brass and V. G. Ambrosia, 1988: Particulate emissions from a mid-latitude prescribed chaparral fire. J. Geophys. Res., 93, 5207–5212.

Crutzen, P. J. and J. W. Birks, 1982: The atmosphere after a nuclear war: twilight at noon. Ambio, 11, 114–125.

Eagan, R. C., P. V. Hobbs and L. F. Radke, 1974: Measurements of cloud condensation nuclei and cloud droplet size distributions in the vicinity of forest fires. J. Appl Meteor., 13, 553–557.

Evans, L. F., I. A. Weeks, A. J. Eccleston and D. R. Packham, 1976: Photochemical ozone in smoke from prescribed burning of forests, Environ. Sci. Tech., 11, 896–900.

Finlayson-Pitts, B. J. and J. N. Pitts, Jr., 1986: Atmospheric Chemistry: Fundamentals and Experimental Techniques, John Wiley & Sons, New York, 1098 pp.

Fuchs, N. A., 1964: The Mechanics of Aerosols, The MacMillan Co., New York, 408 pp.

Gerber, H. E., 1979: A portable cell for simultaneously measuring the coefficients of light scattering and extinction for ambient aerosols, J. Appl. Optics, 18, 1009-1014.

Hegg, D. A., L. F. Radke, P. V. Hobbs, C. A. Brock and P. J. Riggan, 1987: Nitrogen and sulfur emissions from the burning of forest products near large urban areas. J. Geophys. Res., 92, 14,701–14,709.

Hegg, D. A., L. F. Radke, P. V. Hobbs and P. J. Riggan, 1988: Ammonia emissions from biomass burning. Geophys. Res. Let., 15, 335–337.

Hegg, D. A., L. F. Radke, P. V. Hobbs, R. A. Rasmussen and P. J. Riggan, 1990: Emissions of some trace gases from biomass fires. J. Geophys. Res., 95, 5669–5675.

Hobbs, P. V. and L. F. Radke, 1969: Cloud condensation nuclei from forest fires. Science, 183, 279–280.

Johnson, R. L., J. J. Shah, R. A. Cary and J. J. Huntziker, 1981: An automated thermal-optical method for the analysis of carbonaceous aerosol. In Atmospheric Aerosol: Source/Air Quality Measurements, edited by E. S. Marcias and P. K. Hopke, ACS Symposium Series, No. 167, American Chemical Society, Washington, DC, 223–233.

Logan, J. A., 1983: Tropospheric nitrogen oxide budgets. J. Geophys. Res., 88, 10,785–10,807.

Muzio, L. J. and J. C. Kramlich, 1988: An artifact in the measurement of N_2O from combustion sources. Geophys. Res. Letts., 15, 1369–1372.

McMahon, C. K., 1983: Characteristics of forest fuels, fires and emissions. Paper #83-45.1, presented at the 76th Annual Meeting of the Air Pollution Control Association, Atlanta, GA, 19-24 June.

National Academy of Science, 1986: Global Tropospheric Chemistry: Plans for the U.S. Research Effort. National Academy Press, Washington, D.C., 110 pp.

Patterson, E. M. and C. K. McMahon, 1984: Absorption characteristics of forest fire particulate matter. Atmos. Environ., 18, 2541–2551.

Radke, L. F., 1989: Airborne observations of cloud microphysics modified by anthropogenic forcing. In preprints of Symposium on the Role of Clouds in Atmospheric Chemistry and Global Climate, Amer. Meteor. Soc. Annual Meeting, 29 January 3 February 1989, Anaheim, CA, 310–315.

Radke, L. F., A. S. Ackerman, D. A. Hegg, J. H. Lyons, P. V. Hobbs and J. E. Penner, 1991a: Effect of aging on the smoke from a forest fire: implications for the nuclear winter hypothesis. J. Geophys. Res., (Submitted).

Radke, L. F., D. A. Hegg, P. V. Hobbs, J. D. Nance, J. H. Lyons, K. K. Laursen, R. E. Weiss, P. J. Riggan and D. E. Ward, 1991b: Particulate and trace gas emissions from large biomass fires in North America. In Proceedings of the Chapman Conference on Global Biomass Burning: Atmospheric, Climate and Biospheric Implications, 19–23 March 1990, Williamsburg, VA, MIT Press (In press).

Radke, L. F., D. A. Hegg, J. H. Lyons, C. A. Brock, P. V. Hobbs, R. Weiss and R. Rasmussen, 1988: Airborne measurements on smokes from biomass burning. In Aerosols and Climate, P. V. Hobbs and M. P. McCormick, Eds. A. Deepak Publishing Co., 411–422.

Radke, L. F., J. H. Lyons, P. V. Hobbs and R. E. Weiss, 1990. Smokes from the burning of aviation fuel and their self-lofting by solar heating. J. Geophys. Res., 95, 14,071–14,076.

Radke, L. F., J. L. Stith, D. A. Hegg and P. V. Hobbs, 1978: Airborne studies of particles and gases from forest fires. J. Air Poll. Control Assoc., 28, 30–34.

Rasmussen, R. A. and M. A. K. Khalil, 1981: Atmospheric methane (CH_4): Trends and seasonal cycles. J. Geophys. Res., 86, 9826–9832.

Rasmussen, R. A., H. H. Westberg and M. Holdren, 1974: Need for standard referee GC methods in atmospheric hydrocarbon analysis. J. Chrom. Sci., 12, 80–85.

Rasmussen, R. A. and M. A. K. Khalil, 1980: Atmospheric halocarbons: Measurements and analyses of selected trace gases. Proceedings of the NATO Advanced Study Institute on Atmospheric Ozone, A. C. Aikin, Ed., U.S. Department of Transportation.

Rodgers, C. F., J. G. Hudson and J. Hallett, 1990: Cloud droplet nucleation by crude oil smoke and coagulated crude oil/wood smoke particles. Atmos. Environ., 24A, 1–10.

SMIC, 1971: Report of the Study of Man's Impact on Climate, MIT Press.

Stith, J. L., L. F. Radke and P. V. Hobbs, 1981: Particle emissions and the production of ozone and nitrogen oxides from the burning of forest slash. Atmos. Environ., 15, 73–82.

Susott, R. A., D. A. Ward, R. E. Babbit and D. J. Latham, 1991: The measurements of trace emissions and combustion characteristics for a mass-fire. In Proceedings of the Chapman Conference on Global Biomass Burning: Atmospheric, Climate and Biospheric Implications, 19–23 March, 1990, Williamsburg, VA, MIT Press (In press).

Tangren, C. D., 1982: Scattering coefficient and particulate matter concentration in forest fire smoke. J. Air Pollut. Control Assoc., 32, 729–732.

Turco, R. P., O. B. Toon, T. P. Ackerman, J. B. Pollack and C. Sagan, 1983: Nuclear winter: global consequences of multiple nuclear explosions. Science, 222, 1283–1292.

Twomey, S. A., 1977: The influence of pollution on the shortwave albedo of clouds. J. Atmos. Sci., 34, 1149–1152.

Ward, D. E., D. V. Sandberg, R. D. Ottmar, J. A. Anderson, G. C. Hofer and C. K. Fitzsimmons, 1982: Measurements of smokes from two prescribed fires in the Pacific Northwest. Seventy-Fifth Annual Meeting of the Air Pollution Control Association, (Available from D. E. Ward, U.S.D.A. Forest Service, Intermountain Fire Science Laboratory, Missoula, MT 59807).

Ward, D. E., 1990: Factors influencing the emissions of gases and particulate matter from biomass burning. In: Fire in the Tropical Biota, J. G. Goldammer Ed., Springer-Verlag, Heidelbert, (In press).

Ward, D. E. and Hardy, C. C., 1991: Smoke emissions from wildland fires. Environ. Internat., (In press).

Weiss, R. E., A. D. Waggoner, R. J. Charlson, D. A. Thorsell, J. S. Hall and L. A. Richy, 1979: Studies of the optical, chemical and physical properties of light-absorbing aerosols. In Proceedings of the Conference on Carbonaceous Particles in the Atmosphere, LBL-9037, Conf. #7803101, Berkeley, CA, 257–262.

Wornat, M. J. and A. F. Sarofim, 1990: "Char- and aerosol-associated polycyclic aeromatic compounds from coal pyrolysis." Aerosol Sci. and Tech., 12, 832–841.

10. ACKNOWLEDGEMENTS

It is our pleasure to thank the Alaska Fire Service for hosting and assisting us during our stay in Alaska. The support of the Defense Nuclear Agency and the Intermountain Research Station, Forest Service, U.S. Department of Agriculture, is also gratefully acknowledged. Special thanks go to Dr. Darold Ward, Project Leader of the Intermountain Fire Sciences Laboratory, for his considerable input and assistance in both the field study and in the preparation of this report.

APPENDIX A

THE UNIVERSITY OF WASHINGTON'S CONVAIR C-131A RESEARCH AIRCRAFT AND THE INSTRUMENTS USED IN THIS STUDY

General Description of the Aircraft and Pertinent Onboard Instruments

The Convair C-131A is a large twin-engine, propeller driven aircraft that is equipped to carry a sizeable instrumentation payload plus a crew of up to eight people. During our study of the Alaskan wildfire, the crew consisted of a flight scientist, a systems engineer, an aerosol scientist, an atmospheric chemist, a lidar operator, and an OEC/nephelometer operator.

Instruments on board the aircraft, in conjunction with a data processing and display system, make it possible to collect data in each of the following areas: navigational and flight characteristics, general meteorology, cloud physics, aerosol, cloud and atmospheric chemistry, and remote sensing. Detailed information on the instruments used for this study is presented in Table A.1.

TABLE A.1. INSTRUMENTATION ABOARD THE UNIVERSITY OF WASHINGTON'S RESEARCH AIRCRAFT USED DURING THE STUDY OF A BOREAL BIOMASS FIRE IN ALASKA

Parameter	Instrument Type	Manufacturer	Range (and error)
		Aerosol	
Mass concentration particles	Electrostatic deposition onto matched oscillators	Thermal Systems, Inc. Model 3205	0.1 to 3000 $\mu g\ m^{-3}$ ($< 0.2\ \mu g\ m^{-3}$)
Size spectrum of particles	Electric aerosol analyzer	Thermal Systems, Inc. Model 3030	0.0032 to 1.0 μm*
Size spectrum of particles	90° lightscattering	Particle Measuring Systems (LAS-200)	0.5 to 11 μm*
Size spectrum of particles	Forward lightscattering	Royco 245 (In-house modified)	1.5 to 40 μm*
Size spectrum of particles	Diffusion battery	Thermal Systems, Inc. Model 3040 with in-house automatic valves and sequencing	0.01 to 0.2 μm*
Size spectrum of particles	35 - 120° lightscattering	Particle Measuring Systems Model ASASP-X	0.09 to 3.0 μm ($< 0.007\ \mu m$)*
Light-scattering coefficient	Integrating nephelometer	Meteorology Research, Inc. Model 1567 (modified for increased stability and better response time)	$1.0 \times 10^{-6}\ m^{-1}$ to $2.5 \times 10^{-3}\ m^{-1}$
Light-extinction coefficient	Optical extinction cell (2 m path length)	Waggoner Electronics	5×10^{-5} to $10^{-2}\ m^{-1}$
		Atmospheric Chemistry	
Particulate $SO_4^=$, NO_3^-, Cl^-, Na^+, K^+, NH_4^+,	Teflon filters CSI & XRF spectroscopy and Dionex ion exchange chromatography	In-house	0.1 to 50 $\mu g\ m^{-3}$ (for 500 liter air sample)
Gaseous NH_3	Teflon filters followed by filtration with oxalic acid impregnated filters	In-house	(5% – 60% error, depending on filter loading)

* All particle sizes refer to maximum particle dimensions

TABLE A.1. (Continued)

Parameter	Instrument Type	Manufacturer	Range (and error)
	Atmospheric Chemistry (Continued)		
Ozone	Chemiluminescence (C_2H_4)	Monitor Labs Model 8410 A	0 to 5 ppm (< 7 ppb)
NO, NO_2, NO_x	Chemiluminescence (O_3)	Modified Monitor Labs Model 8840	0 to 5 ppm (~ 1 ppb)
CO	Correlation spectrometer	Teco Model 48	0 - 50 ppm (~ 0.1 ppm)
CO_2	Correlation spectrometer	Customized Teco Model 41H	0 - 1000 ppm (~ 4 ppm)